A petrographical and geochemical study of granitoids from the southeastern part of the Linderödsåsen Horst, Skåne

Charlotta Janson

Examensarbete i Geologi vid
Lunds universitet - Berggrundsgeologi, nr. 173

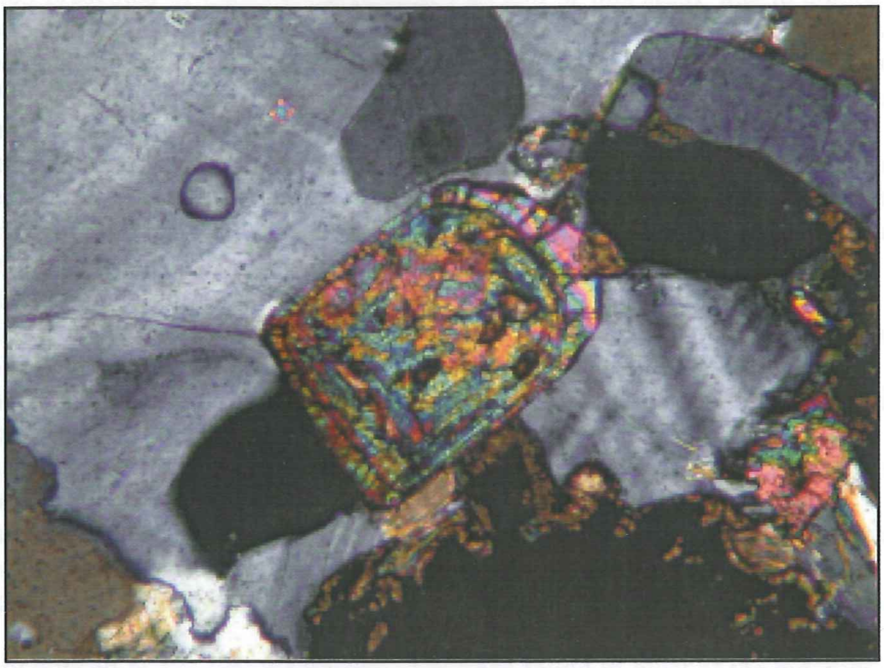

Geologiska institutionen
Centrum för GeoBiosfärsvetenskap
Lunds universitet
2004

L; Lo

A petrographical and geochemical study of granitoids from the southeastern part of the Linderödsåsen Horst, Skåne

Charlotta Janson

Janson, C. A petrographical and geochemical study of granitoids from the south-eastern part of the Linderödsåsen Horst, Skåne. *Examensarbete i Geologi vid Lunds Universitet- Berggrundsgeologi, nr. 173.*

Abstract

The Precambrian crystalline basement in Skåne only outcrops in the large NW striking Horsts that are roughly parallel to the Tornquist Zone. In the south-easternmost part of the Linderödsåsen Horst in SE Skåne, the Stenshuvud porphyritic granitoids previously considered to be Palaeoproterozoic volcanic rocks, have been recently dated to 1458 Ma (Čečys *et al.,* 2002). This indicates that these rocks are coeval with the Karlshamn granitoids in Blekinge as well as other granitoids in southern Sweden. This poses questions regarding the relationship between the granitoids at Stenshuvud and the surrounding rocks. In this study, the area around Sankt Olof, west of Stenshuvud, was mapped in the field and structural, as well as petrographical, investigations were carried out. The main part of the present thesis is a presentation of these new data, which also have been included in the structural-geological map of SE Linderödåsen presented in Čečys *et al.* (2002). The aim of this study was to compare the obtained structural, petrographical and geochemical data with previous work on the Stenshuvud area.

The crystalline bedrock west of Stenshuvud mainly consists of fine-grained, markedly foliated gneisses and weakly foliated fine-grained granitoids. Some of these rocks have a porphyritic texture similar to the one found in the granitoids from Stenshuvud. Thin aplitic, sometimes ptygmatic, veins and younger pegmatites exist in the rocks from both areas. The biotite is phlogopitic in all the analysed samples of fine-grained granites from the study area and in the granites from Stenshuvud. Chemically, the fine-grained granites are all similar to each other, and to the Stenshuvud granites which is particularly true in regard to REE- and other trace-elements. Many features indicate that the fine-grained granites of the study area are of the 'Stenshuvud type'. West of this area, close to the small village of Tåghusa, there is an elongate intrusion composed of fine to medium-grained gneissic granitoids, dated to 1442 Ma (Čečys *et al.,* 2002). In the field, the distinguishing feature of these rocks is the aggregates of mafic minerals that define the foliation. Another difference is the composition of biotite, which is richer in iron than that in the granites further to the east. The chemistry of the rocks from the Tåghusa intrusion, differ somewhat from the easterly granites in regard to the major elements, while the trace elements are similar.

The rocks in an area to the west of the Tåghusa intrusion are gneissic to migmatitic, and vary in composition. They are of unclear origin and might represent remnants of older country rock. Occasionally, the gneisses, and the migmatites, are garnet-bearing: the garnet is Mn-rich in the gneisses.

A more or less pronounced NNW-striking foliation has been found in most of the outcrops of the area, indicating that regional deformation had taken place. The foliation varies from magmatic to migmatitic, and in some cases is mylonitic. The elongate shape of the Tåghusa intrusion, stretching in the same direction as the foliation, is yet another indication that the area was affected by deformation during, and somewhat later than, the ca. 1.46 to 1.44 Ga magmatism.

Charlotta Janson, Department of Geology, GeoBiosphere Science Centre, Lund University, Sölvegatan 12, 223 62 Lund.

En petrografisk och geokemisk studie av granitoider på den sydöstra delen av Linderödsåsen, Skåne.

Charlotta Janson

Janson, C. A petrographical and geochemical study of granitoids from the south-eastern part of the Linderödsåsen Horst, Skåne. *Examensarbete i Geologi vid Lunds Universitet- Berggrundsgeologi, nr. 173.*

Sammanfattning

Den prekambriska, kristallina berggrunden i Skåne är blottad endast i de stora nordvästlstrykande horstar som är ungefär parallella med Tornquistzonen. På den sydostligaste delen av Linderödsåsen i sydöstra Skåne har Stenshuvuds porfyritiska granitoider, som tidigare antogs vara paleoproterozoiska vulkaniter, nyligen daterats till 1458 Ma (Čečys *et al.*, 2002). Detta tyder på att bergarterna är samtida med Karlshamnsgranitoiderna i Blekinge samt andra granitoider i södra Sverige, vilket väcker frågor om förhållandet mellan granitoiderna på Stenshuvud och dess omkringliggande bergarter. I denna studie har området runt St. Olof, väster om Stenshuvud, karterats och strukturella såväl som petrografiska undersökningar har utförts. Den största delen av denna studie är en presentation av dessa nya data, som också är inkluderade i en strukturgeologisk karta över SÖ Linderödsåsen, publicerad i Čečys *et al.* (2002). Syftet med denna studie har också varit att jämföra de insamlade strukturella, petrografiska och geokemiska data med befintliga data från Stenshuvudområdet.

Den kristallina berggrunden väster om Stenshuvud består huvudsakligen av finkorniga, såväl starkt folierade granitoida gnejser som svagt folierade finkorniga granitoider. En del har en porfyritisk textur liknande den som återfinns i granitoider från Stenshuvud. Tunna apliter, som ibland är ptygmatitiska, samt yngre pegmatiter återfinns i båda områdena. Biotiten är flogopitisk i alla prover av finkorniga graniter från det studerade området samt i graniter från Stenshuvud. Kemiskt uppvisar dessa finkorniga graniter stora likheter med varandra, och med Stenshuvudgraniterna, vilket är särskilt tydligt vad gäller REE- och andra spårelement. Mycket tyder på att dessa finkorniga graniter från det studerade området är av "Stenshuvudtyp". Väster om detta område, i närheten av byn Tåghusa, finns det en avlång intrusion bestående av fin- till medelkorniga gnejsiga granitoider, som är daterade till 1442 Ma (Čečys *et al.*, 2002). Det i fält mest utmärkande draget för denna bergart, är de mafiska aggregat som definierar foliationen. En annan skillnad är att biotitens sammansättning är mer järnrik än den är i graniterna längre österut. Kemiskt skiljer sig Tåghusaintrusionen en del från de finkorniga granitoiderna österut, samt dem från Stenshuvud, när det gäller huvudelementen, medan spårelementen uppvisar stora likheter.

Bergarterna i ett område strax väster om Tåghusaintrusionen är gnejsiga till migmatitiska och varierar i sammansättning. De är av okänt ursprung men kan eventuellt representera äldre bergarter inom området. Ibland är gnejserna och migmatiten granatförande: granaten är manganrik i gnejserna.

En mer eller mindre uttalad NNV-strykande foliation har återfunnits i de flesta hällar i området, vilket tyder på att en regional deformation förekommit. Foliationen varierar från att vara magmatisk till att vara migmatitisk och är i något fall mylonitisk. Tåghusaintrusionens avlånga form, utsträckt i samma riktning som foliationen är ytterligare en indikation på att området utsattes för deformation åtminstone under, och strax efter, den magmatism som rådde mellan ca 1.46 och 1.44 Ga.

Charlotta Janson, Geologiska institutionen, Centrum för GeoBiosfärvetenskap, Lunds Universitet, Sölvegatan 12, 220 62 Lund.

Introduction and purpose

The present thesis is a part of the investigations of the Precambrian crystalline basement in Skåne. There, it is largely covered by Phanerozoic sediments; outcrops only exist in the Horsts formed by fault tectonics along the Phanerozoic, NW-striking Tornquist Zone. Although different geophysical methods have been applied to understand crustal structures and compositions of the crystalline rocks, large parts of Skåne's geological history in the Precambrian are still poorly known.

The study area is located in SE Skåne on the Linderödsåsen Horst. There, the crystalline rocks are mainly fine-grained to medium-grained gneisses. Less deformed granitoids of clearly intrusive origin are commonly called 'gneissic granites'. Rocks with a porphyritic appearance, described as coarsened volcanic rocks with a porphyritic structure, exist in the area around Stenshuvud, the south eastern-most part of the Linderödsåsen Horst (Wikman and Bergström, 1987). It has been suggested that these rocks be related to some of the Blekinge rocks, either the older Västanå supracrustals, or the younger ca. 1460 to 1450 Ma Karlshamn group (Wikman and Bergström, 1987; Kornfält and Vaasjoki, 1999). Törnebohm and Hennig (1903) described the Stenshuvud rocks as granites with a porphyritic appearance, and in recent investigations, Čečys *et al.* (2002) also have come to the same conclusion. A radiometric dating on the Stenshuvud granitoids shows that the rocks are ca. 1458 Ma old, and thus coeval with some granites of the above-mentioned Karlshamn group in Blekinge.

The purpose of this study was to investigate the relationships between the Stenshuvud granitoids and the surrounding rocks. The area around Sankt Olof, to the west of Stenshuvud, was chosen for field mapping and structural observations. Samples were taken for petrography and geochemistry. The rocks were analysed with an optical microscope and microprobe to describe textures, minerals and mineral compositions. Powdered samples were prepared for geochemical analyses. The main part of this thesis is a presentation of these new data. The intention is also to compare the obtained structural, petrographical and geochemical characteristics of the granitoid rocks from the study area, with available data from the Stenshuvud area. The obtained data are included in the structural-geological map of the bedrock in SE Skåne presented in Čečys *et al.* (2002).

Regional geology of southern Sweden and recent studies in the area

In Sweden, the Baltic Shield consists mainly of Palaeoproterozoic (2500-1600 Ma) rocks. The crust in the north is oldest, and from there, it is generally younging to the south. The Mezoproterozoic (1600-1000 Ma) crystalline rocks are most abundant in the southern parts of Sweden (Figure 1).

The Transscandinavian Igneous Belt (TIB)

The TIB is composed by intrusive and extrusive ca. 1.80-1.66 Ga, mostly felsic rocks. They can be traced in S. Sweden from Småland to Värmland. Contemporaneous (e.g. 1769±2 Ma and 1767±13 Ma, Kornfält, 1993b), slightly deformed, more mafic varieties of the TIB granites have been found in the county of Blekinge (cf. Johansson and Larsen, 1989; Kornfält, 1996). These, so-called 'gneissic granites' and Tving granitoids, form large massives in the northern and eastern parts of the county. Recent datings of the crystallisation ages of some orthogneisses in 'the Eastern Segment of the Sveconorwegian orogen' (ES) have yielded both similar and slightly younger ages (1674 ±7 Ma, Söderlund *et al.,* 1999; 1627 ±4 Ma, Söderlund *et al.,* 2002).

1.46-1.42 Ga rocks, southern Sweden

The Karlshamn group in the county of Blekinge represents the most known part of the intrusions formed during the ca. 1.46 to 1.42 Ga granitoid magmatism in southern Sweden. It constitutes a relatively large part of the bedrock in Blekinge and includes the Karlshamn, Spinkamåla, and Vånga granites. Several studies have been published, where the dating results on the Karlshamn granites vary between 1445 and 1458 Ma (Kornfält, 1996; Kornfält and Vaasjoki, 1999; Čečys *et al.,* 2003). Furthermore, in Čečys *et al.* (2003), an age difference was noticed between the eastern part (1445 ±11 Ma) and the western part (1426 ±11 Ma) of the Karlshamn pluton. The Vånga granite north of Kristianstad has recently been dated to 1448 ±25 Ma in a U-Th, total Pb model age microprobe study on zircon by Geisler and Schliecher (2000). This method has earlier only been used on minerals with high U, Th and Pb contents, mainly monazite.

The TIB rocks in Småland are also intruded by a few massifs of similar ages. Several new datings have been published in Åhäll (2001), among others, the Götemar and Jungfrun granites were dated to 1452 +11/-9 and 1441 ±2 Ma respectively. These results agree better with the general development in southern Sweden, than did the old Rb-Sr whole rock analyses (e.g. Berg *et al.,* 1983; Åberg, 1986).

Recent datings on secondary zircon and rims of magmatic zircons from orthogneisses in the ES have yielded ages between 1.46 and 1.42 Ga (Söderlund *et al.,* 2002 and Christoffel *et al.,* 1999). Datings on granitic and aplitic dykes also have given similar results (e.g. Söderlund 1996). In the ES, no larger granitic intrusions of that period have been found, however, Söderlund *et al.* (2002) suggest that such could exist deeper in the crust.

The Protogine Zone (PZ)

The PZ (ca. 1200-900 Ma) is an important tectonic structure stretching from Dalarna in the north, Skåne in the south. It is marked by syenitic, granitic and mafic intrusions and narrow zones of foliation (Wikman and Bergström, 1987). The PZ roughly follows the Sveconorwegian frontal deformation zone (SFDZ), separating the strongly deformed and migmatised rocks of the Sveconorwegian orogen, from the less deformed Palaeoproterozoic crust of SE Sweden (Wikman and Bergström, 1983). The exact extension of the PZ in Skåne is hard to define because of the sedimentary cover and faulting along the Tornquist Zone. It can roughly be traced from Görbjörnarp/Lönsboda on Linderödsåsen in north-eastern Skåne to Romeleåsen in the south (Wikman and Bergström, 1983).

Eastern Skåne

In eastern Skåne, the Precambrian rocks are mainly fine-grained grey to red gneisses. They partly originate from deformed and recrystallised granitoids and partly from supracrustals. Fine-grained, quartz-rich gneisses in the northern parts, are likely to be recrystallised sedimentary rocks. Some clearly intrusive, less deformed granitoids are called 'gneissic granites', these are usually more homogeneous and less fine-grained than the gneisses (Wikman and Bergström, 1987). NW-running Phanerozoic diabase dykes penetrate the Precambrian basement parallel to the Tornquist Zone. Large parts of the Precambrian rocks are still unknown because of the rare outcrops.

On the provisional geological map over Skåne, volcanic porphyries are shown in the area of Stenshuvud (Bergström *et al.,* 1988). Recent research (Čečys *et al.,* 2002) has included detailed field mapping, interpretation of geophysical maps, geochemical analyses, petrography and U-Pb dating on zircons. Accordingly, the rocks are fine-grained granites to granodiorites, mainly showing a porphyritic texture. In micro-scale, the 'phenocrysts' are distinguished as aggregates of larger sized feldspars, quartz-grains or mafic minerals- i.e. the rocks are glomeroporphyritic. The rocks are generally foliated, varying from magmatic foliation to strong solid-state deformation. The latter is observed in several shear zones. One distinct shear zone is located in the western part of the Stenshuvud National Park. There the granitic rocks are turned into mica-schists and mylonites (Čečys *et al.,* 2002). Two generations of pegmatitic dykes and aplitic veins crosscut the rocks; the aplitic veins sometimes form beautiful ptygmatic folds. The U-Pb dating on zircons, has yielded an age of 1458 ±6 Ma which corresponds well to the ages of the Karlshamn Group in Blekinge (cf. Kornfält, 1996 and 1999; Čečys *et al.,* 2003).

The study area: macroscopic and microscopic investigations

The study area is roughly outlined by the small villages of Bästekille, Sankt Olof and Tåghusa on SE Linderödsåsen. Outcrops of the crystalline rocks vary from accessible road-cuts to flat surfaces and the rock quality from heavily weathered to almost fresh.

Methods

The rare outcropping complicates the outlining of different rocks hence aeromagnetic maps (SGU, 1998) have been of use, where bodies of rocks producing significantly high magnetic anomalies are easily singled out. The Soil and Ecological map (Esko, 1985) and field notes (SGU, unpublished data) were used to locate outcrops of granitic rocks. Samples were then taken for petrography and geochemistry.

Thin-sections from the different rocks were examined optically under a polarising microscope. Several samples were also analysed with a scanning electron microscope: Jeol, JSM6400 equipped with a Link-EDS system (Lund University, Sweden). The acceleration voltage was set at 18 kV and natural and synthetic minerals have been used as standards. The main minerals of interest were biotite and plagioclase and, if present, amphibole and garnet. All the data are presented in Appendix I.

Results

Field mapping, sampling and petrographic investigations have lead to the sub-division of the crystalline rocks into different groups (Figure 2 and Figures 4-5g). These divisions have mainly been based on rock appearance in outcrops, hand specimens and micro-textures and have been confirmed by mineral- and chemical compositions. Point counting (Appendix II) and plotting of modal compositions in the Streckeisen-diagram (Streckeisen, 1967) have also been used for an approximate classification of the rocks studied (Figure 3). The groups are: **1)** the *fine-grained porphyritic granites (PGs),* occupying the eastern part of the study area. Common features are a sometimes glomero-porphyritic texture, magnesium rich biotites and numerous small inclusions of microcline, biotite, opaques and rutile needles in quartz grains; **2)** the westerly *Tåghusa gneissic granitoids (TGGs)* (in Čečys *et al.,* 2002, referred to as the Tåghusa streaky granitoids). They are easily recognised as granitoids with aggregates of mafic minerals defining the foliation; **3)** fine- to medium-grained *leucogranites*, including both veins in the Tåghusa gneissic granitoids and sample cj14 at the border of the TGG intrusion; **4)** the *country rocks: migmatites, banded gneisses* and *garnet gneisses* occupying the area along the south-western border of the Tåghusa intrusion.

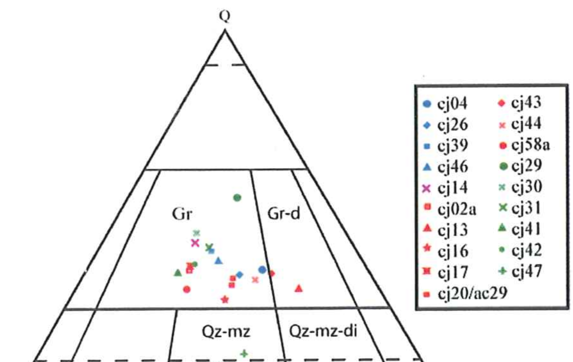

Figure 3. Classifications of the studied rocks (Streckeisen, 1967). Blue (TGGs), purple (leucogranite), green, (country rocks), red (PGs).

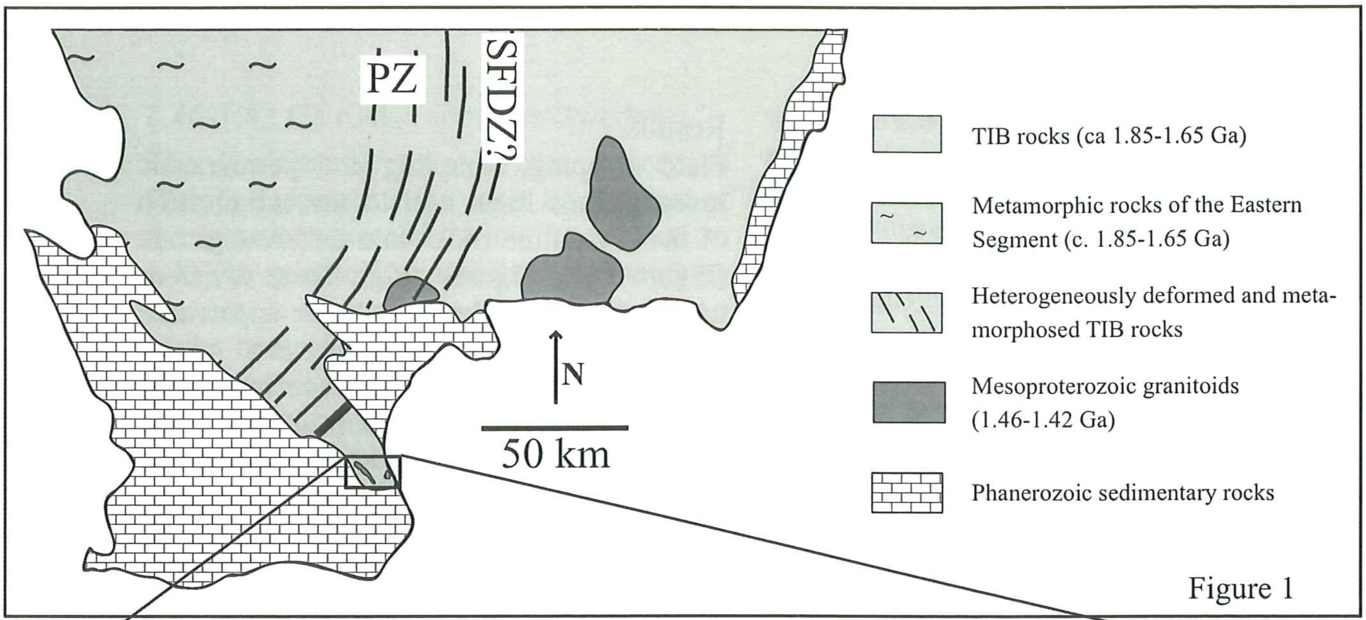

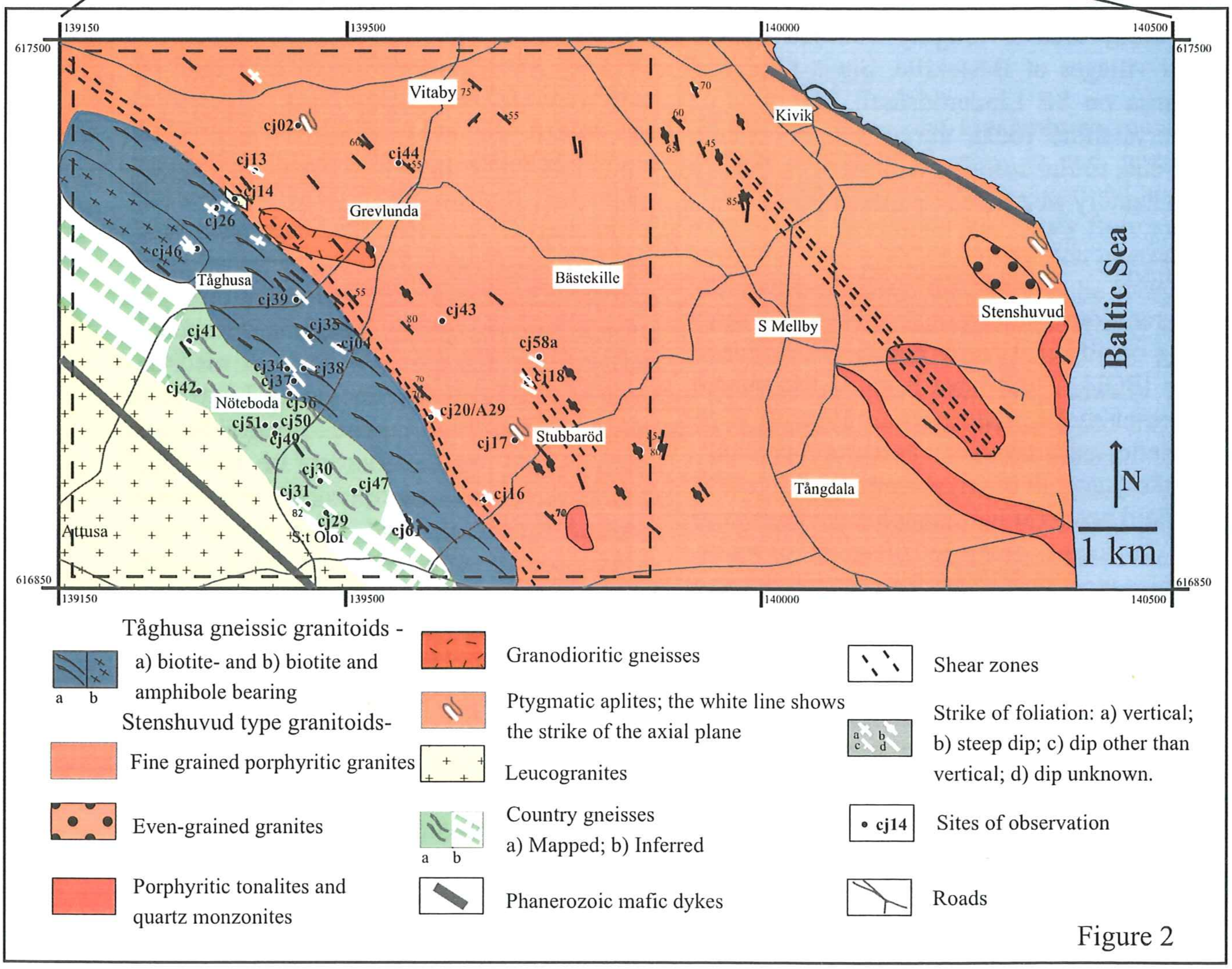

Figure 1. Sketch map of southern Sweden, (modified from Wahlgren *et al.,* 1994 and Söderlund *et al.,* 2002). The black frame shows the location of the study area. PZ (Protogine Zone), SFDZ (Sweconorvegian Frontal Deformation Zone).

Figure 2. Geological map over the study area (roughly outlined by the black dashed frame) and the area east thereof, modified from Cecys *et al.* (2002). White lines represent structural measurements of this study, black lines represent those from Cecys *et al.* (2002).

The porphyritic granites (PGs)

The PGs occupy a large part of the study area, and they are bounded by the TGGs in the west (Figure 2). The PGs are fine-grained and light grey to light red (Figure 4a-d). The PGs change in appearance close to the outlines of the TGGs, for example in a road-cut near Bästekille at the eastern border of the intrusion. There, the rocks show signs of recrystallisation; they are coarser (Figure 4e), foliated and to some extent migmatised. These rocks still contain Mg-rich biotite, indicating that they originally were similar to the PGs in the surrounding area.

Aplitic veins without chilled contacts, some of which are ptygmatic, exist at several localities. Wider pegmatitic dykes are also common.

The main minerals of the PGs are quartz, microcline and plagioclase. Other minerals are biotite, opaques, apatite, zircon, titanite, epidote and rutile. The PGs sometimes have a porphyritic or glomeroporphyritic texture, with aggregates of phenocrysts set in a finer-grained matrix (Figures 5a-c). Generally, the felsic aggregates consist of up to 2.5 mm, anhedral grains of feldspars and some quartz. Mafic aggregates are made up by biotite, opaques and titanite (Figure 5b), large single grains of quartz are also present. The matrix is composed of up to 0.5 mm, anhedral grains of quartz, plagioclase and microcline, and sometimes grains of opaques and biotite. Quartz is more abundant in the matrix than in the felsic aggregates. Thin rims of albite or micro-myrmekite are common between microcline grains and between plagioclase and microcline (Figure 5d).

Some *quartz* grains have numerous inclusions of small (<0.05-0.1 mm) rounded microcline grains, biotite, opaques and needles of rutile (Figure 5e). The *microcline* is often microperthitic containing numerous needle-shaped exsolusions of albite. Some flame-shaped exsolusions appear closer to the grain boundaries. Inclusions are small (0.1-0.2 mm) rounded quartz grains, plagioclase and a small amount of opaques, titanite and biotite. The *plagioclase* varies in composition between An_{23} and An_{28} (Figure 6a). The grains are often partly altered and sometimes they show twinning. The plagioclase contains inclusions of rounded 0.05 to 0.14 mm quartz grains, rounded microcline grains, opaques around which alteration has increased, titanite, and some biotite. The latter is only found in the plagioclase composing the matrix.

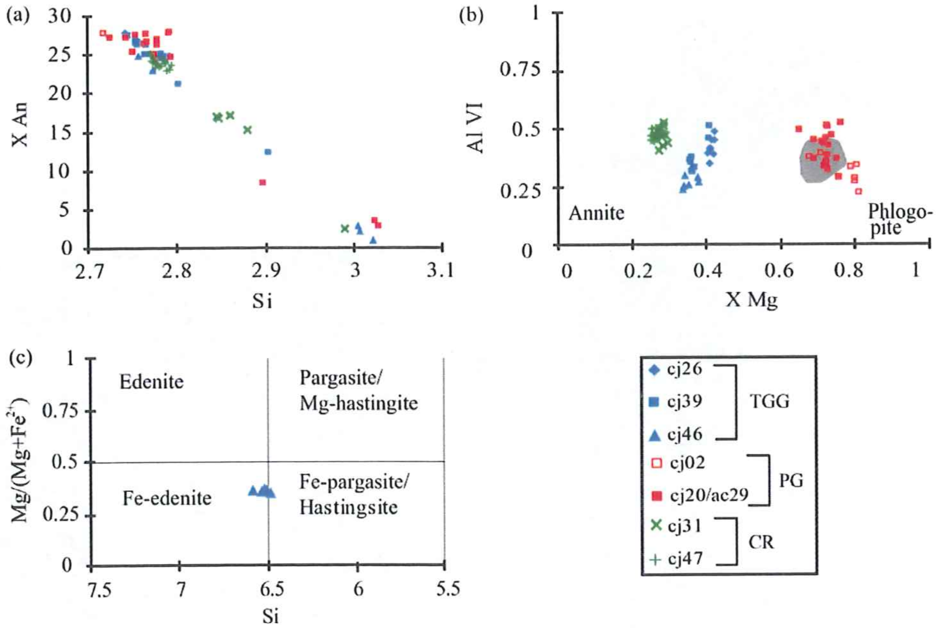

Figure 6. Compositions of rock-forming minerals from the studied rocks: a) Plagioclases from all analysed samples are mainly of oligoclase (An_{10}-An_{30}) composition. Albitic compositions are obtained from clearly visible rims. Similar rims are found in all types of rocks in the study area; b) Diagram showing analysed compositions of biotites from the studied samples. The grey shaded area represents analyses from a Stenshuvud granite (Cecys *et al.*, 2002) for comparison. The magnesium number ($Mg^{2+}/Mg^{2+}+Fe^{2+}$) is plotted on the X-axis, and Al^{VI} per 22 O (Speer, 1984) on the Y-axis; c) Analyses on amphibole from sample cj46. Pargasite- $Al^{VI} \geq Fe^{3+}$, Hastingsite- $Al^{VI} < Fe^{3+}$.

Figure 4. (a)

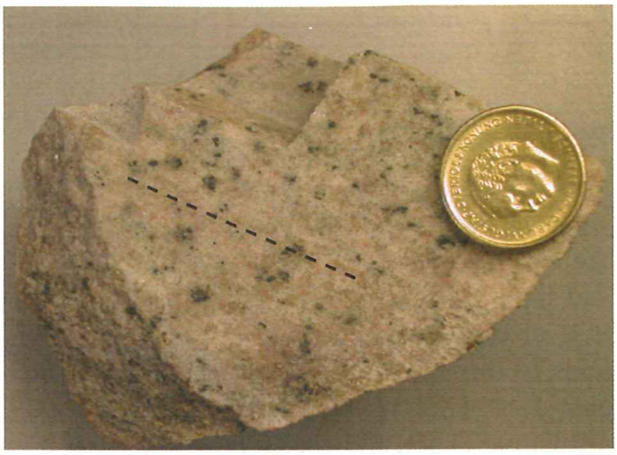

(b)

(c)

(d)

(e)

Figure 4. Fine grained granites of the Stenshuvud type: a) Sample cj02 a relatively even-grained type; b) Sample cj17, a glomeroporphyritic granite; a vague foliation, parallel to the black dashed line, can be distinguished; c) Sample cj16: a very fine-grained porphyritic granite; d) Sample cj20 from an outcrop close to the border of the TGG intrusion; e) Sample cj20b, a more coarse-grained variety from the same outcrop.

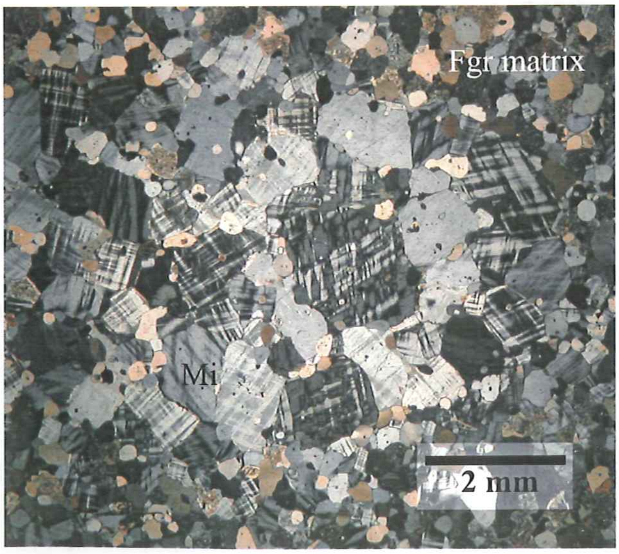

Figure 5. (a)

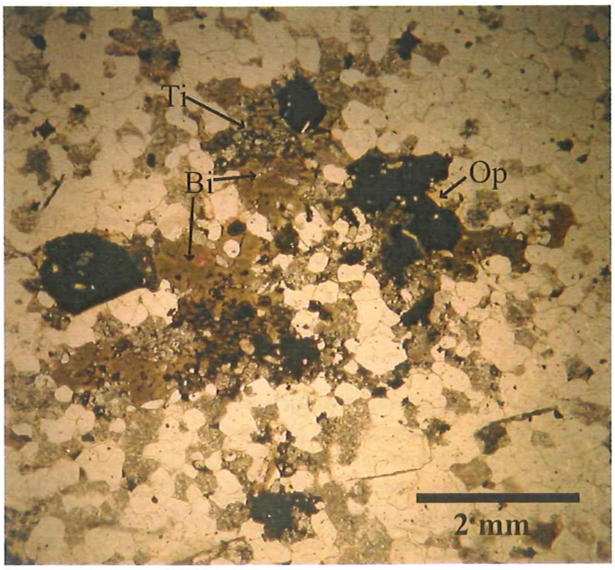

(b)

(Figure 5 continues on the next page)

(Figure 5 continuing)

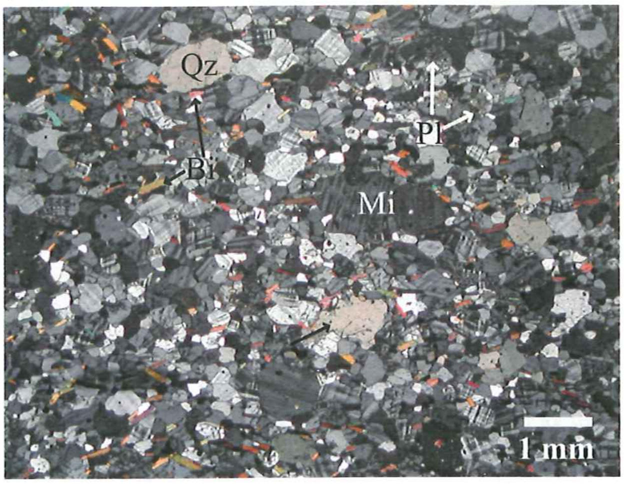

(c)

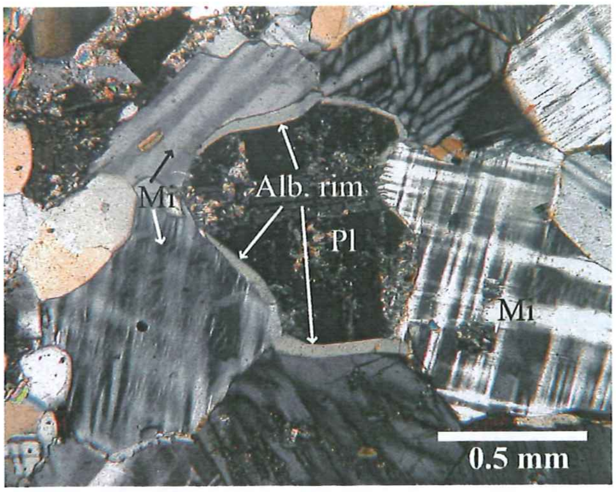

(d)

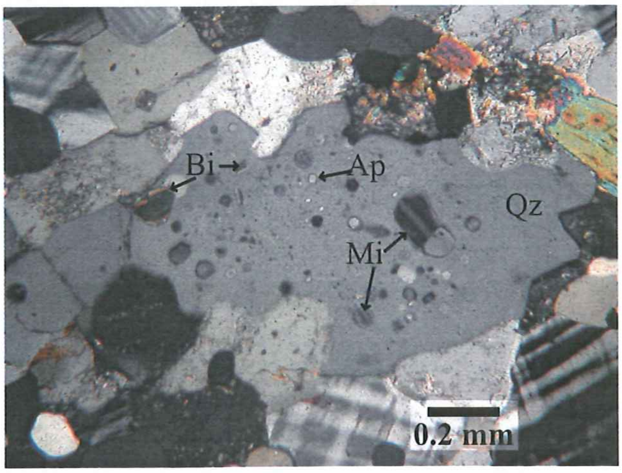

(e)

Figure 5. Examples of microstructures in the fine grained porphyritic granites: a) A microcline aggregate within a fine grained matrix (sample cj17); b) A mafic aggregate composed of biotite, opaque, apatite and titanite (sample cj17); c) A very fine grained porphyritic rock (sampe cj16) with larger crystals of feldspar and quartz. The foliation is defined by aligned biotite flakes. d) Albite rims on a plagioclase grain surrounded by microcline (sample cj20). e) A quartz grain with numerous minute inclusions, often present in the porphyritic granites (sample cj20).

Abbreviations in micro-photographs: Qz (quartz); Mi (microcline); Pl (plagioclase); Amph (Amphibole); Bi (Biotite); Op (opaque); Grt (garnet); Alb (albite); Ti (titanite); Myrm (myrmekite); Sympl (symplektite); Ap (apatite); Chl (chlorite); Def (deformed); Fgr (fine-grained).

Figure 7. (a)

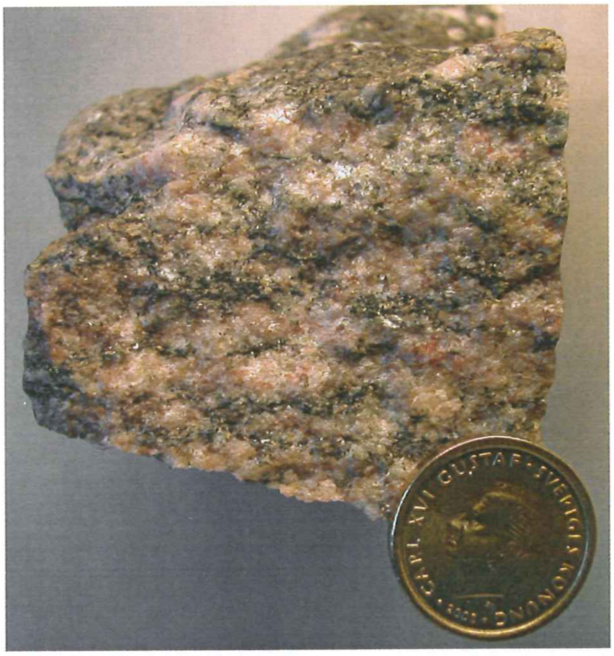

(b)

Figure 7. The Tåghusa gneissic granitoids with aggregates of mafic minerals forming the foliation.
a) The biotite- and hornblende-bearing type (sample cj46);
b) The biotite-bearing type (sample cj26).

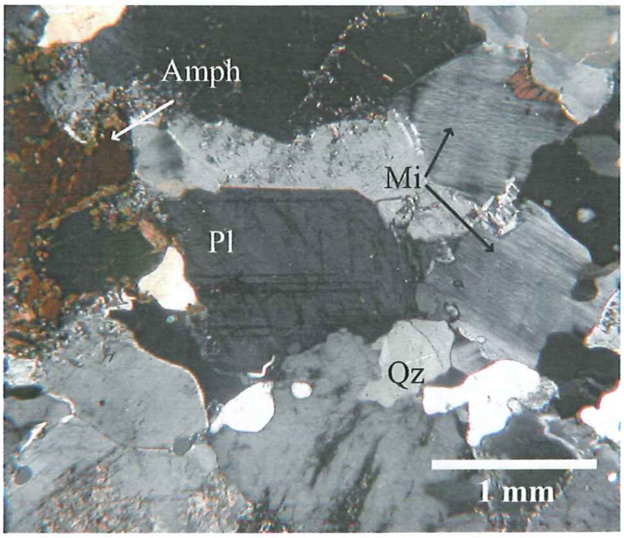

Figure 8. (a)

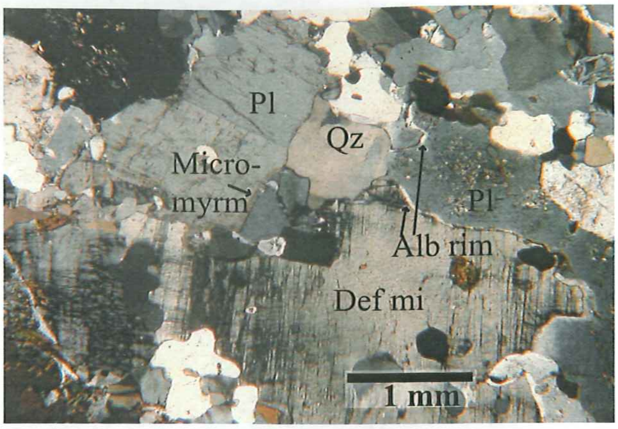

(b)

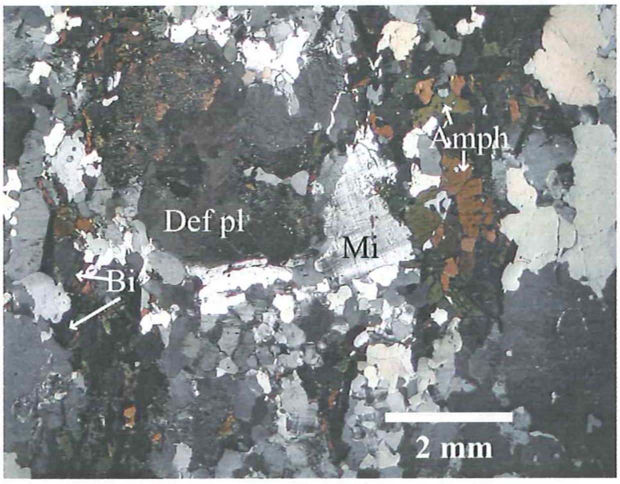

(c)

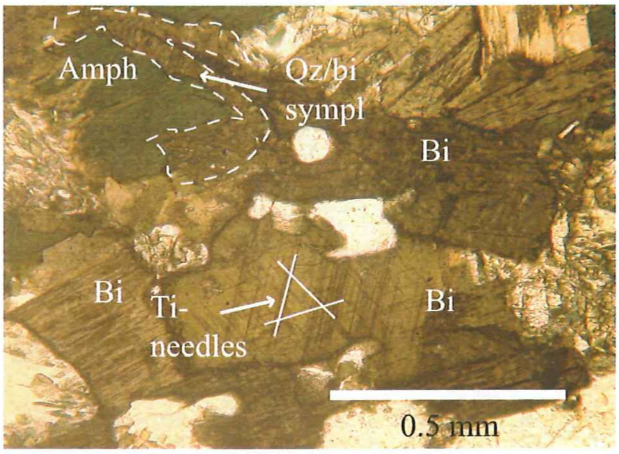

(d)

Figure 8. Microphotographs of the Tåghusa type granitods (sample cj46). a) An aggregate of felsic minerals with preserved magmatic textures; b) Deformed microcline with flame shaped exsolved albites. Thin rims of albite and of myrmekite surrounds plagioclase adjacent to microcline; c) Strongly deformed plagioclase. Aggregates of mafic minerals are also seen; d) Biotite hosting a net of titanite needles (the directions are indicated by thin white lines). See also the symplectite of quartz and biotite that surrounds an amphibole (the area within the dashed lines).

Figure 9.

Figure 9. The leucogranite (sample cj14).

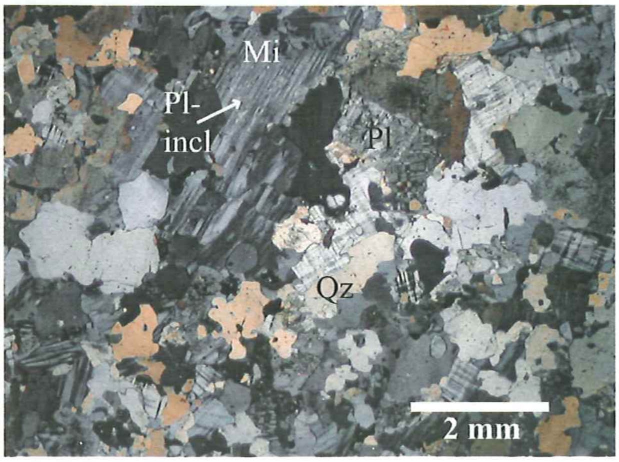

Figure 10.

Figure 10. Microphoto of the leuco-granite (sample cj14). Embaying contacts are seen between several minerals.

Figure 11.

Figure 13.

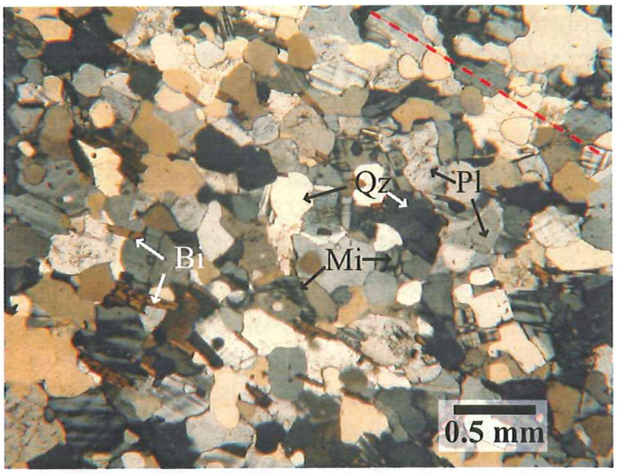

Figure 14a.

Figure 15.

Figure 12.

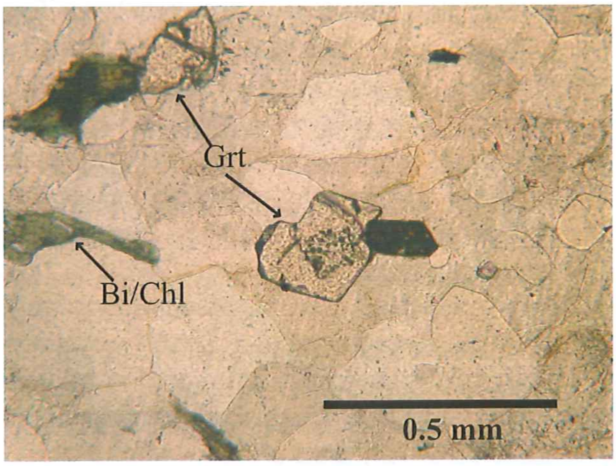

Figure 14b.

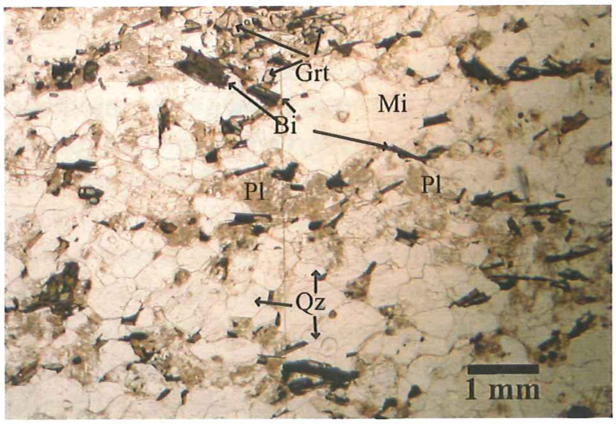

Figure 16.

Figure 11. The migmatite from Nöteboda (sample cj51).

Figure 12. The banded gneiss (sample cj30). Thin bands of leucocratic material are interlayered with grey gneissic parts are seen in the picture.

Figure 13. The granitic garnet-bearing gneiss (sample cj31) with its streaky red-grey pattern.

Figure 14. Micro-photographs of the granitic garnet bearing gneiss. (sample cj31) a) A foliation is defined by flakes of biotite (marked by the red dashed line). b) Subhedral Mn-rich garnets, sometimes with numerous inclusions in the core.

Figure15. The quartz-syenitic garnet-bearing gneiss (sample cj47).

Figure 16. Microphotographs of the same rock showing the foliation defined by alignied minerals. Small anhedral garnet grains are seen in the upper part of the picture.

The *biotite* is phlogopitic, in average [$K_{2.05}$ $Fe_{1.35}$ $Mg_{3.94}$ $Ti_{0.12}$ $Al_{2.39}$ $Si_{5.85}$ O_{20} $(OH)_2$]. Compositional variations are noticed both between samples from different localities and within the samples (Figure 6b). The pleochroic colours vary from light brown to greenish brown and under crossed polars, the colours are bright, which is common for biotites with a high amount of magnesium. Inclusions in the biotite are mostly quartz grains. The *opaque* crystals are large (up to 1.5 mm), anhedral to euhedral and sometimes poikilitic. Apart from the mafic aggregates, it also exists as single grains in the matrix and in felsic aggregates. The *titanite* is most common as rims around opaques but also occurs as rounded 'droplets' together with felsic minerals. *Zircon* is included in biotite and microcline and is associated with the opaques. *Apatite* (up to 1.5 mm) occurs most commonly together with mafic minerals. Anhedral to subhedral crystals of *epidote* are associated with biotite.

The Tåghusa gneissic granitoids (TGGs)

A body of fine- to medium-grained biotite-bearing, and in one known case, biotite- and hornblende-bearing, gneissic granitoids has been found west of the PGs (Figure 2). The presence of these rocks has been established in numerous outcrops. There are several good localities near the small village of Tåghusa, hence the name used for this type of rock. A U/Pb multigrain zircon dating on the hornblende-bearing sample of the TGGs (sample cj46) has given an age of 1442±9 Ma (Čečys *et al.*, 2002).

The TGGs are easily recognised as a large positive high on the magnetic anomaly map (SGU, 1998). From this, the size of the TGG intrusion can be estimated to be approximately 1.5 x 10 km. The anomaly pattern of this high indicates some internal inhomogenities that might be due to the existence of several sub-phases. The TGGs vary in colour from light grey to light red. The most striking feature of the TGGs is the aggregates of mafic minerals that form elongate, sub-parallel domains, and define the foliation in the rocks (Figures 7a and b). Minerals visible in hand specimen are quartz, microcline, plagioclase, biotite, amphibole and opaques. Amphibole exists only in the more mafic part of the granitoids, one of the above-mentioned sub-intrusions.

The TGGs are mostly composed of quartz, microcline, plagioclase, and mafic minerals such as biotite, amphibole (sample cj46) and opaques. Accessory minerals are apatite, zircon, titanite and allanite (sample cj46). Within the mafic aggregates mentioned above, biotite and, when present, amphibole are often aligned sub-parallel or parallel to the foliation. Occasionally, elongate grains of quartz and microcline are also aligned parallel to the foliation. Aggregates of larger sized (up to 4 mm) grains of microcline and plagioclase are also common (Figures 8a-c). Although the magmatic textures with sharp, straight boundaries are sometimes preserved within the felsic aggregates (Figure 8a), their outlines are mostly ragged. The aggregates are separated by a finer grained (ca. 0.5 mm) matrix, where quartz is more abundant than in the felsic aggregates.

Large grains of microcline and some plagioclase exhibit undulose extinction (Figures 8b and c). Quartz exhibits deformation ranging from undulose extinction to subgrains. Zones of very small quartz grains are present in sample cj26. Reaction rims between different minerals are common. Thin rims of albite and very fine myrmekite are common around plagioclase grains bounded to microcline (Figure 8b) and the opaque grains sometimes have a corona of titanite. Micro-symplectitic rims of biotite-quartz and epidote-quartz sometimes replace hornblende in sample cj46 (Figure 8d). Biotite in the same sample is poikilitic and hosts a net of titanite needles, strictly arranged in three directions (Figure 8d).

The *quartz* grains are irregularly shaped. Inclusions are few and are mainly small grains of opaques and fine needles of rutile. The *microcline* is often microperthitic and needle-shaped exsolusions of albite are common. Some exsolusions are, however, flame shaped or patchy. The grains vary in size, and shape but are mostly large and anhedral to subhedral. Inclusions are small (0.05 to 0.4 mm) quartz blebs, plagioclase grains and a few grains of biotite and opaques. The *plagioclase* (An_{21} to An_{27}) (Figure 6a) occurs as anhedral to subhedral, often heavily altered grains. Magmatic, chemical zoning has not been observed. Only a few grains show twinning. Inclusions in the plagioclase are mostly 0.05 to 0.4 mm quartz blebs, but there are also a few grains of microcline, hornblende, biotite and opaques.

The *biotite* has the average composition [$K_{1.98}$ $Fe_{3.12}$ $Mg_{1.98}$ $Ti_{0.23}$ $Al_{2.69}$ $Si_{5.65}$ O_{20} $(OH)_4$] (Figure 6b). The pleochroism is strong and the colour varies from yellow to brownish green. In some samples, biotite is partly altered to chlorite. The *amphibole* [$Na_{0.48}$ $K_{0.27}$ $Ca_{1.93}$ $Fe_{2.99}$ $Mg_{1.64}$ $Ti_{0.17}$ $Al_{1.72}$ $Si_{6.53}$ O_{22} $(OH)_2$ in average] is of ferro-edenitic to ferroan pargasitic composition according to the classification of Leake *et al.* (1997). The composition is constant and does not vary between the rim and the core (Figure 6c). The crystals are anhedral to subhedral, ca. 1 mm and often show the typical amphibole cleavage. This amphibole is strongly pleochroic and the colours vary from olive green to yellow. The crystals are poikilitic and contain rounded quartz grains. **Zircon** is included in the plagioclase and the microcline and occurs together with quartz and mafic minerals.

The leucogranites

A fine-grained, reddish leucogranite (cj14) (Figure 9) has been found in one locality close to the boundary of the Tåghusa intrusion. Some larger grains of quartz, mirrors of feldspars and sometimes opaques can be distinguished in hand specimen. As mentioned above, veins of similar material are also present within the TGGs.

The major minerals in the leucogranite (sample cj14) are quartz, microcline and plagioclase (Figure 10). Opaque minerals: biotite, epidote and zircon compose only ca. 3% of the rock volume. Embaying grain boundaries are common between microcline, plagioclase and quartz grains (Figure 10). Thin rims of albite and myrmekite are common around plagioclase bordering to microcline.

Larger grains of *quartz* exhibit undulose extinction and smaller grains show undulose to straight extinction. Inclusions in quartz are plagioclase, biotite, opaques and zircon. The *microcline* is anhedral and is commonly microperthitic or contains spots of perthite (Figure 10). It often contains inclusions of small rounded quartz grains, angular plagioclase and sometimes biotite or opaques. The *plagioclase* is anhedral to subhedral; the latter is usually seen in smaller grains with good twinning. Some larger grains are also twinned. Inclusions are rounded grains of quartz and opaques. A few plagioclase grains contain spots of microcline, all of them having the same crystallographic direction.

The *biotite* shows pleochroic colours, varying from almost white, to dark green. Biotite is sometimes replaced by chlorite or epidote. *Epidote* also substitutes for altered plagioclase. The *opaques* are anhedral to euhedral. They mostly appear as single grains but in a few cases, they occur together with biotite. Some grains of *zircon* are included in the quartz and microcline.

The country rocks

The term 'country rocks' has been used to cover a group of fine- to medium-grained, gneissic to migmatitic rocks of unknown origin. They might represent remnants of older rocks within the study area. The 'country rocks' are located in a zone following the western boundary of the TGGs and reaching Sankt Olof in the south. Their appearances vary almost from one outcrop to another. They show different degrees of metamorphism, deformation and recrystallisation, from more developed migmatites and banded gneisses, to garnet gneisses. The migmatites and banded gneisses are most common, while the garnet gneisses are only found in two outcrops just north of Sankt Olof. These garnet gneisses are of two different compositions, one is granitic and one is quartz syenitic. A garnet-bearing migmatite is also located close to the small village of Nöteboda.

Migmatites.- The migmatites (Figure 11) are light red to light grey and mostly fine-grained, but vary to medium-grained. The migmatisation varies from stromatic with thin discontinuous stripes of leucosome, elongated parallel to the foliation, to nebulitic with patches of leucosome grading to the gneissic parts of the rock. Quartz, microcline and plagioclase are visible in hand specimen. Garnet grains, up to 20 mm in size characterise the migmatites in outcrops outside Nöteboda. There are no previous records of such large garnets in these areas, and further investigations have been planned.

The compositions and textures of the migmatites vary between the different localities. The main minerals in the migmatites are quartz, microcline and plagioclase. Biotite and opaques are the most common mafic minerals. Some migmatites contain garnet, other have amphibole.

Banded gneisses (sample cj30).- The banded gneisses are dominated by grey, very fine-grained gneissic parts, interlayered with thin bands of light red rock (Figure 12). The minerals are hard to distinguish in hand specimen. The major part of the rock is fine-grained (0.2 - 0.5 mm), with grey gneissic bands mainly composed of quartz, microcline, plagioclase and biotite. Other minerals are opaques and zircon. The foliation in the grey, gneissic part of the rock is defined by subparallel flakes of biotite; other minerals are randomly organised.

The gneissic parts of the rock are interlayered with two types of leucosomes. Both types are aligned with the foliation in the rock. The most common one forms fine-grained, thin, discontinuous stripes texturally similar to the gneissic parts, except the lack of mafic minerals. The other one composes elongate lenses of mainly medium-grained (up to 1.3 mm) microcline but also with some quartz and plagioclase. Larger biotite grains are often associated with this second type of leucocratic domain. Sometimes the leucosomes, particularly of the first type, are associated with thin melanosome layers enriched in dark minerals. Thin rims of albite sometimes occur on plagioclase bordering to microcline, or exist between microcline grains.

The *quartz grains* are small and rounded and mostly exhibit straight extinction. Inclusions in quartz are biotite, opaque minerals and zircon. The *microcline* is sometimes microperthitic. Plagioclase, biotite, and opaques and rounded quartz grains are included in the microcline. The *plagioclase* is anhedral and often altered. It is without twinning and zoning. Inclusions in plagioclase are quartz and opaques. The *biotite* has a strong pleochroism and the colour varies from dark brown to yellow. Biotite is partly altered to chlorite. The *opaque* grains are subhedral to euhedral. Some are included in biotite. *Zircon* is common together with biotite and quartz.

Garnet gneiss, granitic composition (sample cj31).- The very fine-grained garnet gneiss of granitic composition, is found in a locality just north from Sankt Olof. It has a streaky, red-grey pattern (Figure 13) paralleling to the foliation that is defined by single biotite flakes. Feldspar mirrors and mafic minerals can be distinguished in hand specimen.

The major constituents are quartz, microcline and plagioclase; other minerals are biotite, opaques, garnet, epidote and zircon. The main part of the rock is very fine-grained (0.2-0.5 mm), with no particular orientation of the felsic minerals. Flakes of biotite define the foliation in the rock (Figure 14a). Two types of felsic lenses are aligned along with the foliation, contributing to the gneissic appearance of the rock. One type is composed of larger (up to 2 mm), elongate grains of microcline and quartz. The other one is similar to the matrix in texture and composition but lacks mafic minerals.

Most of the *quartz* grains are small and anhedral and have nearly straight extinction (Figure 14a). A few grains are large and elongate, exhibiting slightly undulose extinction. In quartz, the inclusions are few and consist of small grains of biotite, microcline and euhedral grains of opaques. *Microcline* is found as both large grains in felsic domains and small grains in both matrix and felsic domains. The larger grains are commonly perthitic with flame-shaped and patchy patterns. Some of the small grains have no microperthitic exsolusions. Inclusions in the microcline are grains of rounded quartz, plagioclase, biotite, apatite, subhedral opaques and zircon. The *plagioclase* (An_{17}) (Figure 6a) is mainly anhedral, though a few grains are subhedral. It shows some alteration and some grains are twinned. Plagioclase is often more albitic towards the rim, preferably when bordering to microcline. Inclusions are rounded quartz grains, biotite and accessory zircon.

The *biotite* is annitic with the average composition $K_{1.92}$ $(Na_{0.05})$ $Fe_{3.51}$ $Mg_{1.43}$ $Ti_{0.27}$ $Al_{2.95}$ $Si_{5.49}$ O_{20} $(OH)_4$. The magnesium number (Mg^{2+} / Mg^{2+} + Fe^{2+}) ranges from 0.28 to 0.30 and the silica varies between 5.4 and 5.5 (Figure 6b). Biotite is strongly pleochroic and varies from light brown to greenish-brown. Much of the biotite is replaced by chlorite, especially close to garnet grains. The *garnet* is a spessartine, $(Fe_{1.46}$ $Mn_{1.48}$ $Mg_{0.07}$ $Ca_{0.20})$ $Al_{1.95}$ $Si_{2.92}$ O_{12} is a representative analysis. The grains are small (< 0.4 mm) and subhedral to subeuhedral (Figure 14b). Cracks are common, and sometimes the crystals seem broken. Very small inclusions are often seen in the core of the crystals (Figure 14b). *Opaques* are few and subhedral to euhedral. They are sometimes elongated along with the foliation. *Apatite* grains are very small and occur randomly in the rock. *Zircon* is rather common in this rock. It occurs together with quartz, biotite, plagioclase and opaques.

Garnet gneiss, quartz syenitic composition (sample cj47).- A quartz syenitic garnet gneiss (Figure 15) compose one outcrop along the railway ca. 500 m from the granitic gneiss mentioned above. The rock is red, varies from fine- to medium-grained and is at places even coarse-grained. Whereas the coarser parts seem only slightly deformed and might represent the original parts of the rock, the fine-grained parts are foliated. Minerals visible in hand specimen are mainly microcline, plagioclase and biotite. A considerable amount of *fluorite* exists in fissures.

The quartz syenitic garnet gneiss is mainly made up of microcline, plagioclase and quartz. Other minerals are biotite, opaques, garnet, titanite, apatite, epidote and zircon. The coarser parts of the rock have an anhedral, interlobate texture. Quartz and plagioclase are more common in these parts of the rock. Aggregates of subhedral plagioclase grains show magmatic textures. Thin rims of albite and myrmekite occur both where plagioclase borders to microcline and between microcline grains in the coarser parts of the rock.

The grain size in the finer grained rocks varies from 0.2 to 2 mm. The foliation in the fine-grained parts of the rock is mainly defined by biotite flakes. Mineral associations of quartz, plagioclase, and a small amount of anhedral garnet are, however, also aligned as are some elongated mineral grains. The 'matrix' between these zones often shows an interlocking texture, dominated by microcline, but also containing some quartz and plagioclase. Mafic minerals are very rare in the matrix. Thin rims of albite (and sometimes myrmekite) are common on plagioclase bordering to microcline.

The *quartz* is anhedral and shows only slightly undulose extinction. Inclusions in quartz are biotite, sometimes altered to chlorite, and microcline. The *microcline* is often microperthitic and Carlsbader law twins have been found in several thin-sections of this rock. Very large grains of microcline contain inclusions of subhedral plagioclase and irregular quartz grains. Inclusions in smaller grains are rare. The *plagioclase* (An_{23} to An_{26}) (Figure 6a) is anhedral to subhedral and is often heavily altered. Only a few grains show vague twinning. In some cases, plagioclase contains irregular spots of microcline, all showing the same crystallographic directions. Inclusions in plagioclase are quartz, biotite, some apatite and euhedral grains of opaques.

The *biotite* [$K_{1.98}$ ($Na_{0.05}$) $Fe_{3.58}$ $Mg_{1.33}$ $Ti_{0.31}$ $Al_{3.05}$ $Si_{5.42}$ O_{20} $(OH)_4$] (Figure 6b) is often strongly altered to chlorite. *Fluorite* is sometimes located within biotite crystals. The *garnet*, with the representative composition [($Fe_{1.88}$ $Mg_{0.14}$ $Ca_{0.17}$ $Mn_{1.01}$) $Al_{1.98}$ $Si_{2.91}$], occurs as fractured (< 1mm), banana-shaped, anhedral to subhedral crystals in the foliated parts of the rock (Figure 16). Some grains are elongated along with the foliation. *Opaques* are few and anhedral to euhedral.

Structural features of the area

Foliations have been observed in most of the rocks within the study area. Often, it was possible to measure only the strike of the foliation because of the outcrop conditions. The PGs vary from being vaguely foliated with a slight alignment and elongation of minerals or mineral aggregates, to being strongly foliated or even partly migmatised. In cj16, quartz grains in the matrix only shows vague undulatory extinction, and the foliation is defined by aligned biotite flakes.

Strong foliation and migmatisation is concentrated within several shear-zones, for example along the eastern border of the TGGs (locality cj20), and just to the north of Stubbaröd (locality cj18). In other localities (e.g. cj17) elongate aggregates of felsic minerals, define a vague foliation. The foliation within the TGG is more homogenous and is, throughout the rock, defined by aggregates of mafic minerals.

The foliations within the PGs, the TGGs and the country rocks, as well as the strike of the shear zones vary with few exceptions between 300° and 320°. The TGG intrusion also stretches in the same direction.

As mentioned before, the PGs are cross-cut by thin aplitic veins without 'cold' contacts. These sometimes exhibit ptygmatic folds with the axial planes aligned parallel to the prevailing foliation, resembling those in Stenshuvud (cf. Čečys *et al.,* 2002). Wider pegmatitic dykes also exist within the PGs. Coarser segregations and veins of quartz and feldspar, mostly having embaying contacts, are observed in several localities of the TGGs. These segregations sometimes cut the foliation in the gneissic granitoids.

Geochemistry

Methods

Samples of the TGGs (cj26, cj39 and cj46), the PGs (cj02, cj20, cj43 and cj58a) and the country rocks (cj29, cj41 and cj47) and of one leucogranite (cj14), were chosen for geochemical analyses. The samples were crushed and then powdered in a mortar of wolfram carbide. All samples, except two, were sent to the Acme Analytical laboratories Ltd., Canada. There, the analyses for major elements were performed using ICP-ES (Inductive coupled plasma Electro Spectroscopy). Trace elements, including the rare earths, were analysed by ICP-MS (-Mass Spectroscopy). The other two (cj43 and cj58a) were analysed at Svensk Grundämnesanalys AB, Sweden. For major elements and some trace elements, these analyses were performed using ICP-AES (-Atomic Emission Spectroscopy). The other trace elements, including the rare earths, were analysed by ICP-MS. All results are presented in Appendix III

The CIPW-norms have been calculated using the computer program Chemcast (Appendix IV). For the CIPW-norm, the amounts of iron oxides, in the chemical analyses given as Fe_2O_3, are recalculated to FeO and Fe_2O_3, assuming Fe_2O_3 to constitute 15% of the total.

Rock classification and trace element diagrams

All samples have been classified with the PQ classification-diagram (Figure 17a) by Debon and Le Fort (1983). In the other diagrams, only samples of the TGGs, the PGs and the leucogranite cj14 have been plotted. The chemical variations of the major Stenshuvud granites (Čečys *et al.*, 2002) are shown as shaded areas in the background for comparison.

The PQ-diagram (Debon and Le Fort, 1983) displays the 'relative amounts of potassium feldspar and plagioclase' **P** [K - (Na + Ca)] on the X-axis. The amount by weight of quartz **Q** [Si/3 - (K + Na + 2Ca/3)] is plotted on the Y-axis. The values are expressed as grams-atoms x 10^3/100 g of rock. The granitic field corresponds to the granitic, syenogranitic and a part of the monzogranitic field in the Streckeisen-diagram (1967). The adamellitic field represents the remaining part of the monzogranitic field.

In the AB-diagram (Figure 17b) by Debon and Le Fort (1983), the 'aluminous character' **A** [Al - (K + Na + 2Ca)] is represented on the Y-axis. Rocks are called 'peraluminous' when $A > 0$ and 'metaluminous' when $A \leq 0$. The proportional amount by weight of mafic minerals **B** (Fe + Mg + Ti) is presented on the X-axis. The values are expressed in grams-atoms x 10^3/100 g of rock or mineral. Rocks with $B < 38.8$ (< 7 % mafic minerals) are considered to be leucogranites.

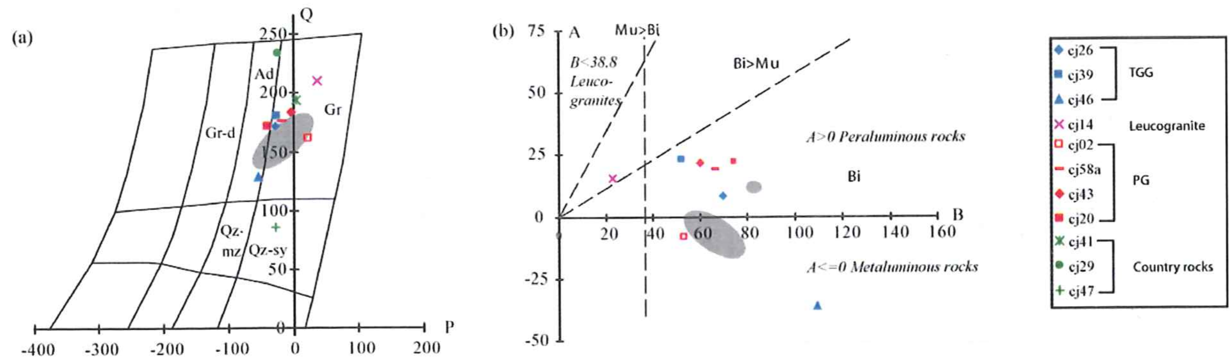

Figure 17. a) The PQ classification-diagram (Debon and Le Fort, 1983) plots the relative amounts of potassium feldspar and plagioclase (P) in the rocks, versus the amounts by weight of quartz (Q). TGG (Tåghusa gneissic granitoids), PG (porphyritic granites), to (tonalite), gr-d (granodiorite), ad (adamellite), gr (granite), qz-mz (quartz-monzonite), qz-sy (quartz-syenite). b) The AB-diagram (Debon, Le Fort, 1983) plots the aluminous character (A) of the rocks, versus the calculated amount of mafic minerals (B).

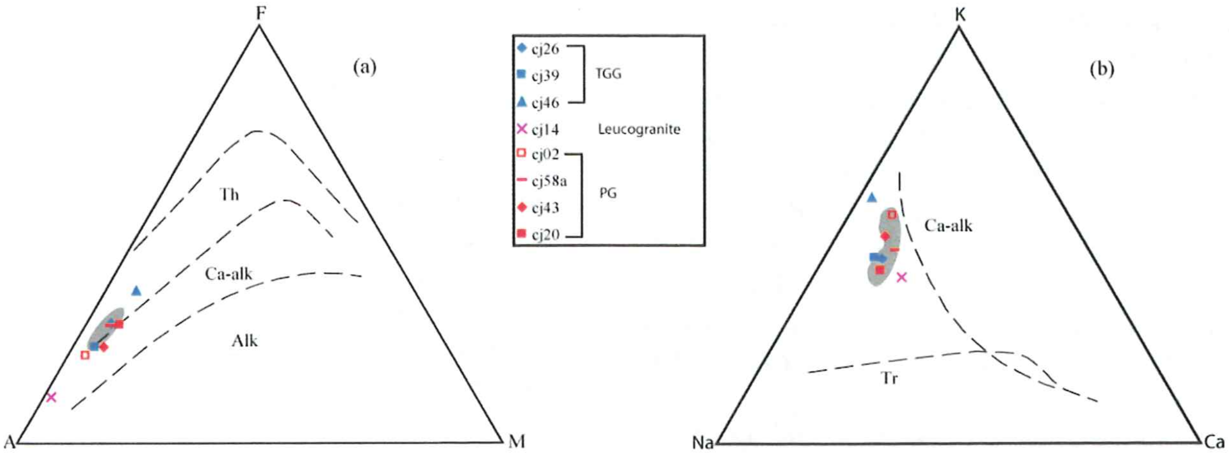

Figure 18. a) The AFM triangular diagram (Kuno, 1968) distinguishing between alkaline, calc-alkaline and tholeiitic rock series. b) Na, K, Ca triangular diagram (Barker and Arth, 1976) discriminating between calc-alkaline and trondhjemitic rock series. Ca-alk (classic calc-alkaline), alk (alkaline), th (tholeiitic).

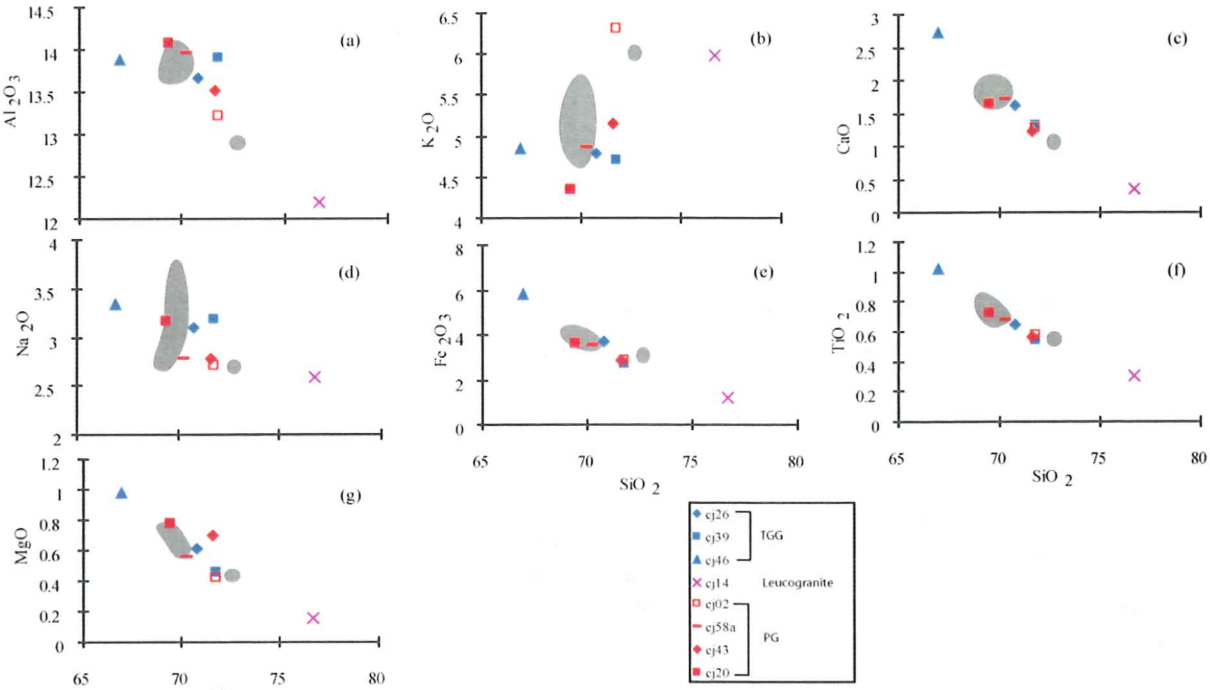

Figure 19a-g. Bivariate diagrams plotting some of the major elements against SiO_2, shaded areas in the background represent the compared Stenshuvud granites.

In the AFM triangular diagram (Figure 18a) by Kuno (1968), A, F and M, respectively represent the oxides $[Na_2O + K_2O]$, $FeO_{total} = [FeO + 0.8998 * Fe_2O_3]$ and MgO in mass %. The triangular diagram plotting the elements Na, K and Ca (Barker and Arth, 1976) has also been used (Figure 18b). Variations in some major elements are shown in the Harker diagrams above (Figure 19a-g).

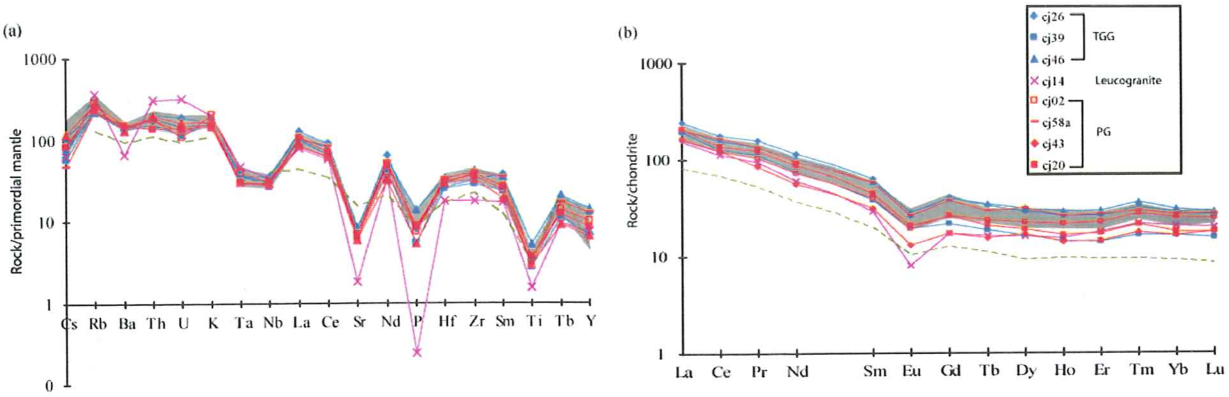

Figure 20. a) Spidergram (normalised to primordial mantle after Wood *et al.,* 1979a; Ti from Wood *et al.,* 1981) b) REE-diagram (normalised to chondrite after Taylor and McLennan, 1985) comparing the TGGs with the PGs. Average upper continental crust (Taylor and McLennan, 1985) is used as a reference line, and the grey area in the background represents the maximum and minimum values for the compared samples from Stenshuvud.

Two types of trace element diagrams have been used for easier comparisons of the different rocks. The values plotted within the spidergram (Figure 20a) are normalised to primordial mantle (Wood *et al.,* 1979a; Ti from Wood *et al.,* 1981). The REE-data (Figure 20b) are normalised to chondrite (Taylor and McLennan, 1985). The fractionation of the REE has been calculated as $(La/Yb)_N$. The Eu anomaly (Eu/Eu*) has been calculated as $[Eu_N/(Sm_N*Gd_N)^{0.5}]$ (Taylor and McLennan, 1985). The composition of the average upper continental crust (AUC by Taylor and McLennan, 1981) has been used as a reference line.

Results

The porphyritic granites

These rocks have a narrow range of SiO_2 content, varying from 69.5 to 71.8 mass % and have been classified as peraluminous adamellites to metaluminous granites (Figure 17a and b). In the AFM-diagram (Figure 18a) they plot close to the A-corner and along the boundary between the calc-alkaline and tholeiitic fields and within the NaKCa-diagram (Figure 18b) they roughly plot along the classic calc-alkaline trend line. The spidergram (Figure 20a) reveals large chemical similarities between the PGs. The most common features in the REE-diagram (Figure 20b) is a sloping trend from La to Eu, a moderate Eu-anomaly (varying between 0.56 and 0.62) and a relatively horizontal to slightly concave pattern for the HREE. Sample cj43 has the steepest slope in the LREE, depending on relatively depleted amounts of the REEs from Pr to Eu. The fractionation of the REE varies between 6.5 and 11.6.

The Tåghusa gneissic granitoids

The TGGs vary in SiO_2 content from 67.0 to 71.8 mass %. They have been classified as metaluminous adamellites to peraluminous granites (Figure 17a and b). In the AFM-diagram (Figure 18a), they plot as marginally calc-alkaline to tholeiitic, and within the NaKCa-diagram (Figure 18b) they roughly follow the classic calc-alkaline trend line. The spidergram (Figure 20a) shows large similarities among the TGG samples. The major feature in the REE-diagram (Figure 20b) is a sloping trend from La to Eu, a moderate Eu anomaly, varying between 0.52 and 0.67, followed by horizontal to slightly concave patterns for the HREE. The fractionation of the REE varies between 6.1 and 11.9 (the highest value is noted in sample cj39). The patterns of sample cj26 and cj46 are almost identical while sample cj39 shows a relative depletion in all REE and records the lowest Eu-anomaly of the TGGs.

The leucogranite

Cj14 has 76.7 mass % SiO_2 and has been classified as a peraluminous leucogranite (Figure 17a and b). It plots close to the A-corner in the AFM diagram (Figure 18a), and close to the classic calc-alkaline trend line in the NaKCa-diagram (Figure 19b). The spidergram (Figure 20a) reveals a strong depletion in Sr and P, some depletion of Ba, Hf, Zr and Ti, as well as increased amounts of Th and U. The REE-diagram (Figure 20b) shows a sloping trend from La to Eu, a rather strong Eu-anomaly (0.35) and some enrichment in the HREE compared to the LREE.

Discussion

Timing of the magmatism

In our recent study (Čečys *et al.,* 2002) the Stenshuvud granites (SGs) were dated to 1458 Ma; the Tåghusa gneissic granitoids (TGGs) from the study area were dated to 1442 Ma, and hence represent a later stage of this magmatism. Several other investigations (e.g. Kornfält, 1999; Åhäll, 2001; Söderlund *et al.,* 2002; Čečys *et al.,* 2003) indicate a similar development in the southern parts of Sweden, with magmatic activity between ca. 1.46 and 1.42 Ga.

Comparison with the Stenshuvud granites

The porphyritic granites (PGs) share many features with the SGs; both rock types are very fine-grained rocks with a sometimes glomeroporphyritic texture. The ca. 20 Ma younger TGGs are coarser than both the PGs and the SGs.

The SGs as well as the PGs contain aplitic veins, of which some are ptygmatic, with the axial planes seemingly parallel to the foliation. This type of folding is mainly considered to result from buckling due to a layer-parallel compression, together with a large vein/rock competence contrast (Twiss and Moores, 1997). Both groups of rock are also cut by a younger generation of pegmatites. The TGGs, on the other hand, contain small leucogranitic veins that sometimes cut the foliation, but lack the larger aplites and pegmatites.

Mineralogical similarities between the PGs and the SGs are the numerous, minute inclusions of rutile and other minerals, mainly in quartz, but also in some feldspar grains while the TGGs have only few mineral inclusions. Microprobe analyses on one sample of the SGs and on several samples of the PGs show that the biotites are of phlogopitic composition and the composition of plagioclase varies between An_{23} and An_{28}. The TGG biotite is richer in iron, and the plagioclase composition varies between An_{21} and An_{27}. The TGGs also have a high amount of magnetite contributing to the strong positive magnetic anomaly recording the TGG intrusion.

The PGs have been classified as peraluminous adamellites to granites while the SGs are metaluminous. The difference in aluminity is mainly due to variations in the amounts of alkalis (K_2O and Na_2O), but also alumina (Figure 19a, b and d). The displaced position of sample cj02 in the Figures 17a and b is mainly due to its high amount of potassium compared with the other samples (Figure 19b). The TGGs are peraluminous to metaluminous adamellites/granites (Figure 17a and b). In the BA-diagram (Figure 17b), the TGGs form a line from the metaluminous sample cj46 to the most peraluminous sample cj39. The major cause for the decreasing A-value from cj26, cj39 to cj46 is an increase in calcium (Figure 19c), while the amounts of Al, K and Na are approximately constant (Figure 19a, b and d).

Both the PGs, the SGs and the TGGs plot along the border between calc-alkaline tholeiitic fields in the AFM-diagram and roughly follow the calc-alkaline trend line in the NaKCa-diagram (Figures 18a and b).

The PGs and the TGGs show very similar features in the REE-diagram and the spidergram (Figure 20a and b). The slightly sloping trend in the LREE, and the flat to slightly concave pattern for the HREE seen in both rock types results in a low (La_N/Yb_N) value. The flat HREE patterns indicate that garnet did not fractionate during the melting of the source rock (Arth, 1976; Irving and Frey, 1978) whereas the slightly concave HREE patterns could possibly indicate a weak fractionation of hornblende (Arth, 1976). As can be seen in the discussion above, there are many indications that the PGs are of the 'Stenshuvud type'.

The leucogranite

The leucograntie (sample cj14) that occurs at the eastern border of the TGG intrusion could represent a late stage in the formation of the TGGs. The low quantities of Fe, Mg and Ti in the leucogranite (Figures 19 e-g), are explained by its low amount of mafic minerals. As can be seen in the spidergram (Figure 20a), the leucogranite has relatively high amounts of Th and U, which is a common feature in restites and pegmatites. Significant troughs can be seen for the elements Ba, P and Sr. The low quantity of mafic minerals could also explain this feature: Ba sometimes substitutes for K in biotites, and Sr can replace Ca in apatite, where P is the other main constituent. Comparing the REEs, the leucogranite largely follows the pattern of the other rocks but has a deeper trough in Eu, than the ones seen in the TGGs and the PGs.

Deformation

A common feature for all rocks within the study area is the uniformly directed foliation, with few exceptions it varies between 300 and 320°. Similar directions are also seen further to the east. The PGs mostly show different degrees of solid state foliation, while both magmatic and solid state foliations are found within the SGs (Čečys *et al.,* 2002). The glomeroporphyritic texture is also better preserved within the SGs. The TGG intrusion is strongly elongated parallel to this regional foliation which is common for intrusions either emplaced during a regional deformation (e.g. Román-Berdiel *et al.,* 1998, Vigneresse, 1995) and/or emplaced within a zone of weakness. Assuming the depth of the body to be no more than ca. 15 km, the volume of the body is consistent with that of rocks intruding in a compressional regime (generally about 200 km^3) (Vigneresse, 1995). The agreement between the foliation directions in the different rocks strongly indicates that a regional tectonic event has affected the study area and areas further to the east.

The characteristic feature of the TGGs (aggregates of mafic minerals defining the foliation) is most common in rocks deformed during metamorphic (i.e. sub-solidus), high-T conditions (Paterson *et al.,* 1989, Paterson *et al.,* 1998, Vernon, 2000). In some cases, however, it also forms during magmatic crystallisation (Paterson *et al.,* 1989). Microstructures show signs of sub-solidus deformation such as undulatory extinction in feldspars and quartz, but lack signs of low-T deformation. The foliation within the intrusion is rather homogenous, also pointing to deformation at higher temperatures (Gapais, 1989). Magmatic foliations together with ductile foliations in rocks further to the east, with similar directions as within the TGGs, point to a deformation coeval with, and slightly postdating, the magmatism. There are few indications of a strong influence on this area by the Sveconorwegian orogeny, which would be the only younger event strong enough to cause the effects seen here. Further investigations including Ar-Ar datings on hornblende or biotite would provide accurate information about the timing of the deformation.

Conclusions

- Two major stages of the Mesoproterozoic granitoid magmatism characterise the study area: they took place at ca. 1.46 Ga (the Stenshuvud porphyritic granites) and at ca. 1.44 Ga, when the Tåghusa granitoids were emplaced. This is coeval with the 1.46 to 1.42 Ga tectonothermal event in other places of southern Sweden.
- The fine-grained porphyritic granites which occupy the area between Stenshuvud and the Tåghusa intrusion. Chemically the porphyritic granites range from slightly metaluminous to peraluminous adamellites and granites; largely following the calc-alkaline trend.
- The westerly Tåghusa granitoids compose a well-defined, elongate intrusive body, which is well constrained by field mapping and magnetic anomalies. These calc-alkaline rocks vary from adamellites to granites and are slightly metaluminous to peraluminous.
- Despite some differences in amounts of major elements, the trace-element patterns, including the REEs of the Tåghusa granitoids and the fine-grained porphyritic granites, as well as the compared Stenshuvud granites, show large similarities, indicating that all these granitoids originated from similar source rocks.
- The porphyritic granites of this study are of the 'Stenshuvud type'.
- Regional deformations, seen as foliations with a strike mainly varying between 300° and 320°, are characteristic of the study area as well as the Stenshuvud area. Other signs of deformation are the ptygmatic aplitic veins existing both within the fine-grained porphyritic granites and within the Stenshuvud granitoids. The porphyritic granites mainly show sub-solidus deformation, which sometimes is enhanced within shear zones. The Tåghusa granitiods are mainly affected by a homogenous sub-solidus deformation and the outlines of the intrusion are parallel to the general foliation in the area.

Acknowledgements

I am grateful and thankful to Svetlana Bogdanova, my supervisor, for all her help, constructive criticism, and encouragement. Thank you Audrius Čečys for your support and collaboration. Thank you to Rickard Anehus for making the thin-sections. Thanks also to Takeshi Miyazu for all the times you have helped me out with the microprobe. Thank you Tania Stanton, for your help to correct and edit this thesis. Thanks to the rest of the staff and fellow students for all the help you have given.

To all my good friends, I am glad that I got to know you, and thanks for all the times you were there when I needed you. I am also very grateful to all those who have helped out when I needed somewhere to stay. Thank you Daniel for your understanding and patience.

This thesis has been performed in cooperation with the international project EUROBRIDGE/EUROPROBE (European Science Foundation) and other research activities on the Precambrian around the Southern Baltic Sea.

References

Arth, J.G., 1976. Behaviour of trace elements during magmatic processes - a summary of theoretical models and their approaches. *Journal of Research of the U.S. Geological Survey 4*, 41-47.

Arth, J.G., Barker F., 1976. Generation of trondhjemitic-tonalitic liquids and Archean bimodal trondhjemite-basalt suites. *Geology 4(10)*, 596-600.

Berg, G., Löfvendahl, R., Levi, B., 1983. Radiometric dating of the Jungfrun granite: *Geologiska Föreningens i Stockholm Förhandlingar 105(3)*, 191-198.

Bergström, J., Kornfält, K.-A., Sivhed, U., Wikman, H. Provisorisk översiktlig berggrundskarta över Skåne. Skala 1:250 000. *Sveriges geologiska undersökning Ba 43.*

Čečys, A., Bogdanova, S., Janson, C., Bibikova, E., Kornfält, K.-A., 2002. The Stenshuvud and Tåghusa granitoids: new representatives of Mesoproterozoic magmatism in southern Sweden. *Geologiska Föreningens i Stockholm Förhandlingar 124*, 149-162.

Čečys, A., Rimsa, A., Johansson, A., Bogdanova, S., 2003. The multiphase Karlshamn pluton, S. Sweden: New Nordsim Zircon ages. *Geophysical Research Abstracts 5.* European Geophysical Society.

Christoffel, C.A., Connelly J.N., Åhäll, K-I., 1999. Timing and characterization of recurrent pre-Sveconorwegian metamorphism and deformation in the Varberg-Halmstad region of SW Sweden. *Precambrian Research 98*, 173-195.

Debon, F., Le Fort, P., 1983. A chemical-mineralogical classification of common plutonic rocks and associations. *Transactions of the Royal Society of Edinburgh: Earth Sciences 73*, 135-149.

Esko, D., 1985. Jordarts- och ekologiska kartan. 2D Tomelilla SO/2E Simrishamn. Skala 1:50 000. *Sveriges geologiska undersöknign Ae 65.*

Gapais, D., 1989. Shear structures within deformed granites: Mechanical and thermal indicators. *Geology 17,* 1144-1147.

Geisler, T., Schleicher, H., 2000. Composition and U-Th-total Pb model ages of polygenetic zircons from the Vånga Granite, South Sweden; an electron microprobe study. *Geologiska Föreningens i Stockholm Förhandlingar 122(2)*, 227-235.

Sveriges Geologiska Undersökning (SGU) 2003. Magnetic anomaly map. Skala 1:400 000.

Geological Survey of Sweden (SGU), 1998. Magnetic anomaly map, 2D Tomelilla SO, 1998 and 2E Simrishamn SV. Scale 1:50 000.

Irving A.J., and Frey, F.A., 1978. Distribution of trace elements between garnet megacrysts and host volcanic liquids of kimberlitic to rhyolitic composition. *Geochimica et Cosmochimica Acta 42*, 771-787.

Johansson, Å., Larsen, O., 1989. Radiometric age determinations and Precambrian geochronology of Blekinge, southern Sweden. *Geologiska Föreningens i Stockholm Förhandlingar 111(1)*, 35-50.

Kornfält, K.-A., 1999. Beskrivning till berggrundskartan 3F Karlskrona NO. Skala 1:50 000. *Sveriges geologiska undersökning Af 199.* 75 pp.

Kornfält, K.-A., Vaasjoki, M., 1999. U-Pb zircon datings of Småland and Karlshamn granites from south-easternmost Sweden; Radiometric dating results 4. *SGU series C 831*, 32-41.

Kornfält, K.-A., 1996. U-Pb zircon ages of six granite samples from Blekinge County, south-eastern Sweden; Radiometric dating results 2, Division of Bedrock Geology Geological Survey of Sweden. *SGU series C 828*, 15-31.

Kornfält, K.-A., 1993. U-Pb zircon ages of three granite samples from Blekinge County, south-eastern Sweden; Radiometric dating results, Division of Bedrock Geology Geological Survey of Sweden. *SGU series C 823*, 17-23.

Kornfält, K-A., Bergström, J., 1983. Beskrivning till berggrundskartan Karlshamn NV. *SGU Af 135*, 173 pp.

Kuno, 1968. Differentiation of basalt magmas. *Interscience, New York Vol. 2*, 623-388.

Leake, B.E., Woolley, A.R., Arps, C.E.S., Birch, W.D., Glibert, M.C., Grice, J.D., Hawthorne, F.C., Akira, K., Kisch, H.J., Krivovichev, V.G., Linthout, K., Laird, J., Mandarino, J.A., Maresch, W.V., Nickel, E.H., Rock, N.M.S., Schumacher, J.C., Smith, D.C., Stephenson, N.C.N., Ungaretti, L., Whittaker, E.J.W., Youzhi, G., 1997. Nomenclature of amphiboles: report of The subcommittee on amphiboles of the international mineralogical association, commission on new minerals and mineral names. *The Canadian Mineralogist 35*, 219-246.

Paterson, S.R., Vernon, R.H., Tobisch, O.T., 1989. A review of criteria for the identification of magmatic and tectonic foliations in granitoids. *Journal of Structural Geology 11(3)*, 349-363.

Paterson, S.R., Fowler, T.K.Jr., Schmidt, K.L., Youshinobu, A.S., Yuan, E.S., Miller, R.B., 1998. Interpreting magmatic fabric patterns in plutons. *Lithos 44*, 53-82.

Román-Berdiel, T., Aranguren, A., Cuevas, J., Tubía, J.M., 1998. Compressional granite-emplacement model: Structural and magnetic study of the Trives Massif (NW Spain). *Lithos 44*, 37-52.

Speer, J.A., 1984. Micas in igneous rocks, *Reviews in mineralogy 13,* 299-356.

Söderlund, U., Möller, C., Andersson, J., Johansson, L., Whitehouse, M., 2002. Zircon geochronology in polymetamorphic gneisses in the Sveconorwegian orogen, SW Sweden: Ion microprobe evidence for 1.46-1.42 and 0.98-0.96 Ga reworking. *Precambrian Reserarch 113* (3-4) 193-225.

Söderlund, U., Jarl, L.-G., Persson P.-O., Stephens M.B., Wahlgren, C.-H., 1999. Protolith ages and timing of deformation in the eastern, marginal part of the Sveconorwegian orogen, south-western Sweden. *Precambrian research 94*, 29-48.

Söderlund, U., 1996: Conventional U-Pb dating versus single-grain Pb evaporation dating of complex zircons from a pegmatite in the high-grade gneisses of south-western Sweden. *Lithos, 38(1-2)*, 93-105.

Taylor, S.R., and McLennan, S.M., 1985. The continental crust: its composition and evolution. Blackwell, Oxford. 312 pp.

Taylor S.R., and McLennan, S.M., 1981. The composition and evolution of the continental crust: rare earth element evidence from sedimentary rocks. Philosophical *Transactions of The Royal Society: Mathematical, Physical and Engineering Sciences A301*, 381-399.

Twiss, R.J., Moores, E.M., 1997. *Structural geology*. W.H. Freeman and company. New York. 532 pp.

Törnebohm, A. E., Hennig, A., 1903. Beskrifning till blad 1 & 2 omfattande de topografiska kartbladen Landskrona, Lund, Kristianstad, Malmö, Ystad, Simrishamn. *Sveriges Geologiska undersökning* Aa 1 & 2.

Vernon, R.H., 2000. Review of micro structural evidence of magmatic and solid-state flow. *Electronic Geosciences 5:2* , 1-24.- Original paper. Department of earth and planetary sciences and ARC Key Centre for the Geochemical evolution and Metallogeny of Continents (GEMOC), Macquarie University, Sydney, NSW 2109, Australia.

Vigneresse, J.L., 1995. Control of granite emplacement by regional deformation. Tectonophysics 249, 173-186.

Wikman, H., Bergström, J., 1987. Beskrivning till provisoriska översiktliga berggrundskartan Malmö. *Sveriges Geologiska undersökning Ba 40*, 42 pp.

Wood, D.A., Joron, J.L., Treuil M., Norry, M., and Tarney, J., 1979. Elemental and Sr isotope variations in basic lavas from Iceland and the surrounding ocean floor.

Contributions to Mineralogy and Petrology 70, 319-339.

Wood, D.A., Tarney, J., and Weaver B.L., 1981. Trace element varitations in Atlantic ocean basalts and Proterozoic dykes from Northwest Scotland: their bearing upon the nature and geochemical evolution of the upper mantle. *Tectonophysics 75*, 91-112.

Åberg., G, 1986. Further radiometric dating of some young granites and a Smaland dike porphyry in south-eastern Sweden. *Geologiska Föreningens i Stockholm Förhandlingar 108(1)*, 57-61.

Åhäll, K.I., nov 2001. Åldersbestämning av svårdaterade bergarter i sydöstra Sverige. *Svensk Kärnbränslehantering AB R-01-60 (ISSN 1402-3091)*, 1-28.

AppendiX I. Microprobe analyses of minerals from the studied rocks

Min- mineral; n.a.- not analysed; n.d.- not detected; Pl- plagioclase; Alb- rim albite; Bi- biotite; Bi-sympl- biotite in symplektite;
Amph- amphibole; Grt- garnet; Tit- titanite; An= Na/(Na+Ca) in %; X Mg =Mg/(Mg+Fe)

Min.	oxide/element Analyse nb.	SiO_2	Al_2O_3	Na_2O	CaO	K_2O	FeO	MgO	TiO_2	MnO	Tot.	O	Si	Al	Na	Ca	K	Fe	Mg	Ti	Mn	An	X Mg	Tot.
	Tåghusa gneissic granitoids																							
	cj26:13	60.67	24.01	7.69	5.36	0.12	0.12	n.d.	n.d.	n.d.	97.97	8	2.74	1.28	0.67	0.26	0.01	<0.01	n.d.	n.d.	n.d.	27.84	-	4.96
	cj26:14	61.05	23.90	7.66	5.12	0.23	0.06	n.d.	n.d.	0.06	98.07	8	2.76	1.27	0.67	0.25	0.13	<0.01	n.d.	n.d.	<0.01	26.94	-	5.07
	cj39:11	61.90	23.67	8.21	4.97	0.25	0.16	n.d.	n.d.	n.d.	99.15	8	2.76	1.25	0.71	0.24	0.01	0.01	n.d.	n.d.	n.d.	25.11	-	4.98
	cj39:13	62.43	23.50	8.10	4.74	0.10	0.22	n.d.	0.05	n.d.	99.14	8	2.79	1.24	0.70	0.23	0.01	0.01	n.d.	<0.01	n.d.	24.46	-	4.97
	cj39:14	64.95	21.77	9.06	2.29	0.03	0.01	n.d.	n.d.	n.d.	98.11	8	2.90	1.15	0.78	0.11	<0.01	<0.01	n.d.	n.d.	n.d.	12.30	-	4.94
	cj39:15	62.88	23.28	8.58	4.16	0.11	0.09	n.d.	0.02	n.d.	99.12	8	2.80	1.22	0.74	0.20	0.01	<0.01	n.d.	<0.01	n.d.	21.17	-	4.97
	cj39:16	61.31	23.48	8.01	4.86	0.08	0.17	n.d.	0.03	n.d.	97.93	8	2.77	1.25	0.70	0.24	<0.01	0.01	n.d.	<0.01	n.d.	25.11	-	4.96
	cj39:17	61.73	24.11	7.89	5.28	0.17	0.10	n.d.	0.10	0.05	99.42	8	2.75	1.27	0.68	0.25	0.01	<0.01	n.d.	<0.01	<0.01	26.95	-	4.97
	cj39:18	61.71	24.20	8.10	5.31	0.12	0.11	n.d.	n.d.	n.d.	99.54	8	2.75	1.27	0.70	0.25	0.01	<0.01	n.d.	n.d.	n.d.	26.62	-	4.99
	cj39:19	62.49	23.55	7.89	4.73	0.10	0.13	n.d.	n.d.	0.02	98.90	8	2.79	1.24	0.68	0.23	0.01	0.01	n.d.	n.d.	<0.01	24.86	-	4.95
	cj39:20	62.14	23.63	7.85	4.77	0.11	0.16	n.d.	0.02	0.01	98.70	8	2.78	1.25	0.68	0.23	0.01	0.01	n.d.	<0.01	<0.01	25.14	-	4.95
	cj39:21	62.66	23.74	8.02	4.74	0.10	0.17	n.d.	0.01	0.01	99.45	8	2.78	1.24	0.69	0.23	0.01	0.01	n.d.	<0.01	<0.01	24.59	-	4.95
	cj39:22	62.79	24.07	8.07	5.24	0.22	0.15	n.d.	n.d.	n.d.	100.53	8	2.77	1.25	0.69	0.25	0.01	0.01	n.d.	n.d.	n.d.	26.39	-	4.97
	cj39:23	62.12	24.04	8.11	5.25	0.24	0.18	n.d.	0.04	n.d.	99.97	8	2.76	1.26	0.70	0.25	0.01	0.01	n.d.	<0.01	n.d.	26.32	-	4.98
	cj39:24	61.01	24.07	7.91	5.43	0.26	0.15	n.d.	0.05	n.d.	98.87	8	2.75	1.28	0.69	0.26	0.02	0.01	n.d.	<0.01	n.d.	27.52	-	5.00
	cj46:18	60.96	23.70	8.23	4.93	0.11	0.09	n.d.	0.02	n.d.	98.03	8	2.76	1.26	0.72	0.24	0.01	<0.01	n.d.	<0.01	n.d.	24.90	-	4.99
	cj46:19	61.80	23.59	8.46	4.56	0.16	0.08	n.d.	0.03	n.d.	98.68	8	2.77	1.25	0.74	0.22	0.01	<0.01	n.d.	<0.01	n.d.	22.93	-	4.98
	cj46:1	69.61	20.47	10.02	0.50	0.07	0.14	n.d.	0.03	0.02	100.86	8	3.00	1.04	0.84	0.02	<0.01	0.01	n.d.	<0.01	<0.01	2.67	-	4.91
Alb	cj46:2	69.44	20.41	9.95	0.37	0.09	0.05	n.d.	0.07	n.d.	100.38	8	3.00	1.04	0.84	0.02	0.01	<0.01	n.d.	<0.01	n.d.	2.00	-	4.90
	cj46:3	69.87	20.01	10.32	0.15	0.05	0.08	n.d.	0.05	n.d.	100.53	8	3.02	1.02	0.86	0.01	<0.01	<0.01	n.d.	<0.01	n.d.	0.80	-	4.91
Bi	cj26:1	35.49	14.24	0.07	n.d.	9.97	22.06	8.75	2.01	1.00	93.59	11	2.83	1.34	0.01	n.d.	1.01	1.47	1.04	0.12	0.07	-	0.41	7.89
	cj26:2	35.55	14.41	0.06	n.d.	9.88	22.15	8.63	1.92	0.98	93.59	11	2.84	1.36	0.01	n.d.	1.01	1.48	1.03	0.12	0.07	-	0.41	7.89
	cj26:3	35.91	14.53	0.18	0.05	9.89	22.14	9.15	1.58	0.91	94.33	11	2.84	1.35	0.03	<0.01	1.00	1.46	1.08	0.09	0.06	-	0.42	7.91
	cj26:4	36.35	14.78	0.23	n.d.	9.83	22.04	9.23	1.44	1.05	94.94	11	2.85	1.39	0.04	n.d.	0.98	1.45	1.08	0.09	0.07	-	0.43	7.94
	cj26:5	35.76	14.82	0.04	n.d.	10.14	22.25	8.80	1.71	0.87	94.38	11	2.82	1.38	0.01	n.d.	1.02	1.47	1.04	0.10	0.06	-	0.41	7.89
	cj26:6	35.67	14.66	0.17	n.d.	9.87	21.73	8.85	1.66	0.90	93.52	11	2.84	1.38	0.03	n.d.	1.00	1.45	1.05	0.10	0.06	-	0.42	7.91
	cj26:8	35.68	14.68	0.12	0.01	9.80	22.13	8.91	1.77	0.96	94.05	11	2.83	1.37	0.02	<0.01	0.99	1.47	1.05	0.11	0.06	-	0.42	7.90
	cj26:9	35.92	14.76	0.13	n.d.	9.94	21.85	9.12	1.55	0.86	94.13	11	2.84	1.38	0.02	n.d.	1.00	1.45	1.08	0.09	0.06	-	0.43	7.92
	cj39:3	36.87	15.61	0.10	0.01	9.96	22.39	8.87	1.76	0.82	96.39	11	2.83	1.42	0.02	<0.01	0.98	1.44	1.02	0.10	0.05	-	0.41	7.85
	cj39:4	36.29	14.95	0.15	0.10	9.70	22.27	8.77	1.76	0.68	94.66	11	2.84	1.38	0.02	0.01	0.97	1.46	1.02	0.10	0.05	-	0.41	7.85
	cj39:5	35.63	14.87	0.05	n.d.	9.98	24.32	7.74	2.19	0.75	95.52	11	2.80	1.38	0.01	n.d.	1.00	1.60	0.91	0.13	0.05	-	0.36	7.87
	cj39:6	35.48	14.70	0.15	0.01	9.62	24.01	7.79	2.12	0.82	94.68	11	2.81	1.37	0.02	<0.01	1.00	1.59	0.92	0.13	0.06	-	0.37	7.89
	cj39:7	35.46	14.70	0.24	0.01	9.55	24.09	7.73	2.31	0.83	94.92	11	2.80	1.37	0.04	<0.01	0.96	1.59	0.91	0.14	0.06	-	0.36	7.86
	cj39:8	35.87	14.61	0.13	n.d.	9.98	23.57	7.89	2.69	0.75	95.49	11	2.81	1.35	0.02	n.d.	1.00	1.54	0.92	0.16	0.05	-	0.37	7.85
	cj39:9	36.20	14.53	0.07	n.d.	10.05	23.97	7.88	2.83	0.66	96.18	11	2.82	1.33	0.01	n.d.	1.00	1.56	0.91	0.17	0.04	-	0.37	7.84
	cj39:10	36.40	14.68	0.09	0.04	10.01	24.20	7.89	2.78	0.82	96.90	11	2.81	1.34	0.01	<0.01	0.99	1.57	0.91	0.16	0.05	-	0.37	7.85
	cj46:6	35.49	14.01	0.10	0.05	9.68	26.16	7.85	1.49	0.35	95.18	11	2.83	1.31	0.02	0.00	0.98	1.74	0.93	0.09	0.02	-	0.35	7.93
	cj46:7	35.37	13.93	0.12	0.08	9.57	26.11	7.68	1.99	0.44	95.29	11	2.81	1.31	0.02	0.01	0.97	1.74	0.91	0.12	0.03	-	0.34	7.91
	cj46:16	35.63	13.76	0.15	n.d.	9.70	24.07	8.47	2.14	0.39	94.31	11	2.84	1.29	0.02	n.d.	0.99	1.60	1.01	0.13	0.03	-	0.39	7.90

App. I cont.

Min.	oxide/element	SiO_2	Al_2O_3	Na_2O	CaO	K_2O	FeO	MgO	TiO_2	MnO	Tot.	O	Si	Al	Na	Ca	K	Fe	Mg	Ti	Mn	An	X Mg	Tot.
											Tåghusa granitoids cont.													
Min.	cj46:32	35.70	14.68	n.d.	n.d.	9.45	25.46	8.42	0.38	0.42	94.49	11	2.84	1.38	n.d.	n.d.	0.96	1.69	1.00	0.02	0.03	-	0.37	7.92
	cj46:8	36.13	13.91	0.14	0.55	9.69	26.34	7.72	1.98	0.48	96.94	11	2.83	1.28	0.02	0.05	0.97	1.72	0.90	0.12	0.03	-	0.34	7.92
	cj46:26	35.73	13.96	0.18	n.d.	9.78	24.20	8.42	2.11	0.36	94.74	11	2.83	1.31	0.03	n.d.	0.99	1.61	1.00	0.13	0.02	-	0.38	7.91
Bi-sympl.	cj46:s7	36.83	14.17	0.13	n.d.	10.13	26.90	8.40	1.53	0.28	98.37	11	2.84	1.29	0.02	n.d.	0.99	1.73	0.96	0.09	0.02	-	0.36	7.94
	cj46:s8	37.61	13.84	0.06	0.02	9.99	26.02	8.46	1.17	0.37	97.55	11	2.90	1.26	0.01	0.00	0.98	1.68	0.97	0.07	0.02	-	0.37	7.90
Amph	cj46:1	41.78	9.47	1.63	11.52	1.30	22.33	7.21	1.48	0.69	97.41	23	6.53	1.75	0.50	1.93	0.26	2.92	1.68	0.17	0.09	-	0.37	7.55
	cj46:4	42.09	9.45	1.62	11.61	1.41	22.69	7.01	1.44	0.79	98.10	23	6.54	1.73	0.49	1.93	0.28	2.95	1.62	0.17	0.10	-	0.36	7.54
	cj46:9	41.74	9.32	1.65	11.55	1.36	22.72	7.09	1.53	0.69	97.65	23	6.52	1.72	0.50	1.93	0.27	2.97	1.65	0.18	0.09	-	0.36	7.60
	cj46:11	41.35	9.39	1.55	11.56	1.39	23.08	6.97	1.48	0.69	97.45	23	6.49	1.74	0.47	1.94	0.28	3.03	1.63	0.18	0.09	-	0.35	7.62
	cj46:5	41.83	9.54	1.61	11.66	1.44	22.75	6.94	1.46	0.68	97.90	23	6.52	1.75	0.49	1.95	0.29	2.97	1.61	0.17	0.09	-	0.35	7.56
	cj46:10	42.16	9.30	1.56	11.45	1.35	23.10	7.20	1.46	0.67	98.23	23	6.55	1.70	0.47	1.91	0.27	3.00	1.67	0.17	0.09	-	0.36	7.57
	cj46:12	41.98	8.94	1.27	11.53	1.22	22.84	7.13	1.49	0.60	97.00	23	6.60	1.66	0.39	1.94	0.25	3.00	1.67	0.18	0.08	-	0.36	7.50
Ti	cj46:a	30.32	4.49	0.09	28.55	0.56	1.74	0.17	34.25	0.03	100.19	3	0.60	0.10	<0.01	0.60	0.01	0.03	0.01	0.51	<0.01	-	-	1.86
	cj46:b	30.76	4.42	0.01	29.07	0.35	1.47	0.05	34.52	0.10	100.76	3	0.60	0.10	<0.01	0.61	0.01	0.02	<0.01	0.51	<0.01	-	-	1.85
	cj46:d	31.12	6.37	n.d.	28.13	0.68	2.19	0.45	30.84	n.d.	99.79	3	0.61	0.15	n.d.	0.59	0.02	0.04	0.01	0.46	n.d.	-	-	1.87
	cj46:X	30.72	4.23	0.06	25.82	1.33	3.55	1.14	32.64	0.04	99.52	3	0.61	0.10	<0.01	0.55	0.03	0.06	0.03	0.49	<0.01	-	-	1.87
	cj46:e	30.12	4.07	n.d.	29.03	0.23	1.48	0.06	34.45	0.05	99.51	3	0.60	0.10	n.d.	0.61	0.01	0.02	<0.01	0.51	<0.01	-	-	1.85
	cj46:m	30.14	3.18	0.06	27.64	0.72	2.03	0.42	35.64	0.13	99.95	3	0.59	0.07	<0.01	0.58	0.02	0.03	0.01	0.53	<0.01	-	-	1.85

Porphyritic granites of the Stenshuvud type

Min.	oxide/element Analyse nb.	SiO_2	Al_2O_3	Na_2O	CaO	K_2O	FeO	MgO	TiO_2	MnO	Tot.	O	Si	Al	Na	Ca	K	Fe	Mg	Ti	Mn	An	X Mg	Tot.
Pl	cj02:1	59.35	23.22	8.00	5.62	0.79	1.17	n.d.	0.02	n.d.	98.17	8	2.72	1.25	0.71	0.28	0.05	0.05	n.d.	<0.01	n.d.	27.89	-	5.05
	cj02:10	61.88	23.53	8.13	4.68	0.09	0.14	n.d.	0.03	n.d.	98.48	8	2.78	1.24	0.71	0.23	0.01	0.01	n.d.	<0.01	n.d.	24.14	-	4.96
	cj02:11	61.64	23.98	7.72	5.04	0.12	0.11	n.d.	0.01	n.d.	98.62	8	2.76	1.27	0.67	0.24	0.01	n.d.	n.d.	<0.01	n.d.	26.51	-	4.95
	cj20:22	60.50	24.15	7.90	5.48	0.16	0.22	n.d.	n.d.	0.03	98.45	8	2.75	1.30	0.70	0.27	0.01	0.01	n.d.	n.d.	<0.01	27.70	-	5.03
	cj20:23	60.62	24.25	7.92	5.38	0.19	0.10	n.d.	n.d.	0.08	98.54	8	2.74	1.29	0.70	0.26	0.01	n.d.	n.d.	n.d.	<0.01	27.30	-	5.00
	cj20:24	61.51	23.82	8.38	4.97	0.09	0.10	n.d.	0.02	n.d.	98.89	8	2.79	1.28	0.74	0.24	0.01	n.d.	n.d.	<0.01	n.d.	24.69	-	5.05
	cj20:27	60.52	24.12	8.01	5.45	0.13	0.20	n.d.	0.02	0.01	98.46	8	2.72	1.28	0.70	0.26	0.01	0.01	n.d.	<0.01	<0.01	27.34	-	4.98
	cj20:28	61.23	23.77	8.22	4.98	0.16	0.12	n.d.	0.04	0.04	98.55	8	2.77	1.27	0.72	0.24	0.01	n.d.	n.d.	<0.01	<0.01	25.10	-	5.02
	cj20:29	60.57	24.10	7.94	5.48	0.17	0.19	n.d.	n.d.	0.07	98.51	8	2.75	1.29	0.70	0.27	0.01	0.01	n.d.	n.d.	<0.01	27.64	-	5.03
Alb	cj02:19	64.81	21.97	8.97	1.47	0.51	0.15	n.d.	n.d.	n.d.	97.88	8	2.90	1.16	0.78	0.07	0.03	0.01	n.d.	n.d.	n.d.	8.26	-	4.93
Pl	ac29-b:18	61.05	24.34	8.04	5.40	0.11	0.17	n.d.	n.d.	n.d.	99.11	8	2.78	1.31	0.71	0.26	0.01	0.01	n.d.	n.d.	n.d.	27.06	-	5.07
	ac29-b:19	61.12	23.82	7.87	5.20	0.21	0.13	n.d.	0.02	n.d.	98.35	8	2.77	1.27	0.69	0.25	0.01	0.01	n.d.	<0.01	n.d.	26.75	-	5.00
	ac29-b:20	61.63	23.85	8.05	4.97	0.07	0.12	n.d.	n.d.	n.d.	98.69	8	2.75	1.26	0.70	0.24	n.d.	0.01	n.d.	n.d.	n.d.	25.48	-	4.94
	ac29-b:21	61.01	24.24	7.66	5.38	0.20	0.20	n.d.	n.d.	n.d.	98.69	8	2.79	1.31	0.68	0.26	0.01	0.01	n.d.	n.d.	n.d.	27.97	-	5.06
	ac29-b:23	61.47	23.95	7.83	5.08	0.19	0.22	n.d.	n.d.	0.05	98.79	8	2.78	1.28	0.69	0.25	0.01	0.01	n.d.	n.d.	<0.01	26.39	-	5.01
	ac29-b:26	60.82	23.94	7.77	5.45	0.14	0.29	n.d.	0.06	n.d.	98.46	8	2.79	1.29	0.69	0.27	0.01	0.01	n.d.	<0.01	n.d.	27.95	-	5.06
	ac29-b:28	60.73	24.14	7.91	5.50	0.21	0.23	n.d.	0.02	n.d.	98.74	8	2.77	1.30	0.70	0.27	0.01	0.01	n.d.	<0.01	n.d.	27.74	-	5.05
Alb.	ac29-b:27	66.77	20.07	10.11	0.64	0.09	0.05	n.d.	0.04	n.d.	97.76	8	3.02	1.07	0.89	0.03	0.01	n.d.	n.d.	<0.01	n.d.	3.38	-	5.01
	ac29-b:29	67.75	20.18	9.98	0.50	0.03	0.11	n.d.	n.d.	0.01	98.56	8	3.02	1.06	0.86	0.02	n.d.	n.d.	n.d.	n.d.	<0.01	2.70	-	4.97

App. I cont.

Min.	oxide/element	SiO_2	Al_2O_3	Na_2O	CaO	K_2O	FeO	MgO	TiO_2	MnO	Tot.	O	Si	Al	Na	Ca	K	Fe	Mg	Ti	Mn	An	X Mg	Tot.
	Analyse nb.										Porphyrtitic granites cont.													
Bi	cj02:12	39.10	13.85	0.06	0.01	10.07	11.63	16.23	1.09	1.12	93.16	11	2.96	1.23	0.01	<0.01	0.97	0.74	1.83	0.06	0.07	-	0.71	7.87
	cj02:13	39.82	13.41	0.04	n.d.	10.75	8.23	18.98	1.12	1.48	93.83	11	2.96	1.17	0.01	n.d.	1.02	0.51	2.10	0.06	0.09	-	0.80	7.92
	cj02:14	39.76	13.51	0.15	0.02	10.56	8.14	18.92	1.16	1.49	93.71	11	2.95	1.18	0.02	<0.01	1.00	0.51	2.09	0.07	0.09	-	0.81	7.92
	cj02:20	38.97	13.97	0.03	n.d.	10.34	12.82	15.50	1.23	1.13	93.98	11	2.94	1.24	<0.01	n.d.	1.00	0.81	1.74	0.07	0.07	-	0.68	7.88
	cj02:27	39.96	13.31	0.15	0.05	10.36	7.89	19.53	1.23	1.42	93.89	11	2.95	1.16	0.02	<0.01	0.98	0.49	2.15	0.07	0.09	-	0.82	7.89
	cj02:29	39.96	13.50	0.01	0.32	10.07	8.37	18.12	1.28	1.53	93.16	11	2.98	1.18	<0.01	0.03	0.96	0.52	2.01	0.07	0.10	-	0.79	7.84
	cj02:30	40.21	13.88	0.25	0.02	10.52	7.96	19.01	1.02	1.17	94.04	11	2.96	1.21	0.04	<0.01	0.99	0.49	2.09	0.06	0.07	-	0.81	7.89
	cj20:5	38.17	13.83	0.36	0.01	10.07	13.66	14.52	1.23	1.42	93.26	11	2.97	1.27	0.06	<0.01	1.00	0.89	1.69	0.07	0.09	-	0.65	8.04
	cj20:9	38.72	13.45	0.06	n.d.	10.22	12.72	16.19	1.20	0.54	93.10	11	2.97	1.21	0.01	n.d.	1.00	0.81	1.85	0.07	0.04	-	0.69	7.95
	cj20:10	38.83	13.70	0.01	0.01	10.50	12.70	16.30	1.29	0.64	93.97	11	2.98	1.24	<0.01	<0.01	1.03	0.82	1.86	0.08	0.04	-	0.70	8.04
	cj20:11	39.07	13.43	0.14	0.01	10.39	11.53	16.90	1.45	0.85	93.76	11	3.00	1.21	0.02	<0.01	1.02	0.74	1.93	0.08	0.06	-	0.72	8.06
	cj20:12	39.07	13.66	0.10	0.02	10.35	10.97	17.18	1.34	1.17	93.86	11	2.98	1.23	0.02	<0.01	1.01	0.70	1.95	0.08	0.08	-	0.74	8.04
	cj20:13	39.64	13.55	0.11	0.03	10.53	11.32	17.36	1.44	0.71	94.69	11	2.96	1.19	0.02	<0.01	1.00	0.71	1.93	0.08	0.05	-	0.73	7.94
	cj20:15	39.25	13.65	0.09	n.d.	10.73	11.28	17.39	1.25	0.85	94.47	11	2.97	1.22	0.01	n.d.	1.04	0.71	1.96	0.07	0.05	-	0.73	8.03
	cj20:16	40.03	13.61	0.04	n.d.	10.56	11.19	18.14	1.18	1.23	95.98	11	3.02	1.21	0.01	n.d.	1.02	0.71	2.04	0.07	0.08	-	0.74	8.14
	ac29-b:1	39.36	13.66	0.13	n.d.	10.64	11.40	17.31	1.14	1.25	94.89	11	2.96	1.21	0.02	n.d.	1.02	0.72	1.94	0.06	0.08	-	0.73	8.01
	ac29-b:2	39.50	14.10	0.13	0.01	10.35	11.23	17.05	1.06	1.36	94.79	11	2.99	1.26	0.02	<0.01	1.00	0.71	1.93	0.06	0.09	-	0.73	8.05
	ac29-b:3	39.42	13.76	0.16	n.d.	10.65	11.26	17.20	1.36	1.30	95.09	11	3.01	1.24	0.02	n.d.	1.04	0.72	1.96	0.08	0.08	-	0.73	8.15
	ac29-b:5	39.09	13.31	0.13	n.d.	10.50	11.59	17.38	1.37	1.00	94.38	11	2.98	1.20	0.02	n.d.	1.02	0.74	1.97	0.08	0.07	-	0.73	8.07
	ac29-b:6	39.15	13.52	0.03	n.d.	10.64	11.44	17.38	1.20	0.93	94.30	11	2.96	1.21	0.01	n.d.	1.03	0.72	1.96	0.07	0.06	-	0.73	8.01
	ac29-b:10	42.17	14.26	0.11	n.d.	10.48	10.41	19.37	0.76	0.78	98.33	11	3.04	1.21	0.02	n.d.	0.96	0.63	2.08	0.04	0.05	-	0.77	8.04
	ac29-b:15	41.26	13.91	0.06	n.d.	10.69	10.61	19.14	1.55	1.08	98.29	11	2.96	1.18	0.01	n.d.	0.98	0.64	2.05	0.08	0.07	-	0.76	7.96
	ac29-b:17	39.57	13.26	0.13	n.d.	10.58	10.25	17.97	1.47	1.04	94.26	11	3.00	1.18	0.02	n.d.	1.02	0.65	2.03	0.08	0.07	-	0.76	8.05
	ac29-b:31	39.47	13.75	0.07	n.d.	10.59	11.49	16.74	1.78	1.18	95.07	11	2.95	1.21	0.01	n.d.	1.01	0.72	1.87	0.10	0.08	-	0.72	7.94
	ac29-b:32	39.26	13.96	n.d.	n.d.	10.58	11.28	16.77	1.59	1.22	94.65	11	2.98	1.25	n.d.	n.d.	1.02	0.72	1.90	0.09	0.08	-	0.73	8.02
	ac29-b:37	39.65	13.78	0.11	0.25	10.40	11.74	16.70	1.28	1.19	95.11	11	2.99	1.23	0.02	<0.01	1.00	0.74	1.88	0.07	0.08	-	0.72	8.00

App. I cont.

Country gneisses

Min.	oxide/element Analyse nb.	SiO_2	Al_2O_3	Na_2O	CaO	K_2O	FeO	MgO	TiO_2	MnO	Tot.	O	Si	Al	Na	Ca	K	Fe	Mg	Ti	Mn	An	X Mg	Tot.
Pl	cj31:39	64.22	22.57	8.90	3.24	0.17	0.05	n.d.	0.14	0.01	99.29	8	2.85	1.18	0.77	0.15	0.01	<0.01	n.d.	0.01	<0.01	16.76	-	4.96
	cj31:42	65.51	22.29	8.92	2.92	0.19	0.10	n.d.	n.d.	0.02	99.93	8	2.88	1.15	0.76	0.14	0.01	<0.01	n.d.	n.d.	<0.01	15.27	-	4.94
	cj31:43	64.22	22.75	8.85	3.28	0.23	0.10	n.d.	n.d.	n.d.	99.43	8	2.84	1.19	0.76	0.16	0.01	<0.01	n.d.	n.d.	n.d.	17.03	-	4.96
	cj31:45	65.05	22.71	8.89	3.34	0.20	0.09	n.d.	n.d.	0.05	100.32	8	2.86	1.18	0.76	0.16	0.01	<0.01	n.d.	n.d.	<0.01	17.16	-	4.96
	cj31:46	69.06	20.85	9.99	0.43	0.04	0.16	n.d.	0.02	n.d.	100.55	8	2.99	1.06	0.84	0.02	n.d.	0.01	n.d.	<0.01	n.d.	2.33	-	4.91
	cj31:47	65.16	22.78	8.77	3.29	0.17	0.17	n.d.	n.d.	n.d.	100.34	8	2.86	1.18	0.75	0.15	0.01	0.01	n.d.	n.d.	n.d.	17.13	-	4.95
	cj47:9	61.94	23.30	8.15	4.67	0.19	0.14	n.d.	0.03	n.d.	98.41	8	2.79	1.24	0.71	0.23	0.01	0.01	n.d.	<0.01	n.d.	24.04	-	4.98
	cj47:10	63.33	23.82	8.42	4.65	0.29	0.22	n.d.	n.d.	n.d.	100.73	8	2.78	1.23	0.72	0.22	0.02	0.01	n.d.	n.d.	n.d.	23.40	-	4.97
	cj47:11	63.30	23.85	8.12	4.54	0.14	0.10	n.d.	n.d.	0.01	100.07	8	2.79	1.24	0.70	0.22	0.01	<0.01	n.d.	n.d.	<0.01	23.63	-	4.95
	cj47:12	62.10	23.49	7.91	4.67	0.14	0.11	n.d.	0.03	n.d.	98.46	8	2.78	1.24	0.69	0.22	0.01	<0.01	n.d.	<0.01	n.d.	24.59	-	4.94
	cj47:13	61.84	23.78	7.87	4.80	0.12	n.d.	n.d.	0.06	0.02	98.49	8	2.77	1.26	0.68	0.23	0.01	n.d.	n.d.	<0.01	<0.01	25.19	-	4.95
	cj47:15	61.53	23.59	7.95	4.86	0.14	0.07	n.d.	0.07	0.02	98.24	8	2.77	1.25	0.69	0.23	0.01	<0.01	n.d.	<0.01	<0.01	25.24	-	4.96
	cj47:20	62.28	23.32	8.27	4.49	0.14	0.04	n.d.	0.02	0.01	98.56	8	2.79	1.23	0.72	0.22	0.01	<0.01	n.d.	<0.01	<0.01	23.10	-	4.97
	cj47:21	61.76	23.64	8.26	4.73	0.16	0.12	n.d.	n.d.	0.01	98.68	8	2.77	1.25	0.72	0.23	0.01	<0.01	n.d.	n.d.	<0.01	24.00	-	4.98
	cj47:24	61.71	23.52	8.18	4.50	0.14	0.08	n.d.	0.05	n.d.	98.18	8	2.78	1.25	0.71	0.22	0.01	<0.01	n.d.	<0.01	n.d.	23.31	-	4.96
	cj47:25	63.32	23.90	8.40	4.78	0.14	0.08	n.d.	n.d.	n.d.	100.62	8	2.79	1.24	0.72	0.23	0.01	<0.01	n.d.	n.d.	n.d.	23.91	-	4.97
	cj47:26	63.25	24.06	8.36	4.84	0.13	0.07	n.d.	0.05	0.02	100.78	8	2.77	1.24	0.71	0.23	0.01	<0.01	n.d.	<0.01	<0.01	24.20	-	4.96
	cj47:27	63.41	23.84	8.44	4.54	0.12	0.21	n.d.	0.04	n.d.	100.60	8	2.79	1.24	0.72	0.21	0.01	0.01	n.d.	<0.01	n.d.	22.94	-	4.97
	cj47:28	63.84	24.35	8.46	4.76	0.14	0.07	n.d.	0.10	n.d.	101.73	8	2.78	1.25	0.71	0.22	0.01	<0.01	n.d.	<0.01	n.d.	23.74	-	4.97
	cj47:29	63.47	24.01	8.40	4.71	0.13	0.15	n.d.	0.06	n.d.	100.92	8	2.78	1.24	0.71	0.22	0.01	0.01	n.d.	<0.01	n.d.	23.66	-	4.96
	cj47:33	62.68	23.89	8.18	4.57	0.20	0.06	n.d.	n.d.	n.d.	99.58	8	2.78	1.25	0.70	0.22	0.01	<0.01	n.d.	n.d.	n.d.	23.56	-	4.96
	cj47:35	62.38	23.76	8.18	4.61	0.16	0.11	n.d.	n.d.	n.d.	99.19	8	2.78	1.25	0.71	0.22	0.01	<0.01	n.d.	n.d.	n.d.	23.76	-	4.96
	cj47:36	61.74	23.69	8.22	4.77	0.31	0.13	n.d.	0.05	n.d.	98.89	8	2.77	1.25	0.72	0.23	0.02	0.01	n.d.	<0.01	n.d.	24.26	-	4.99
	cj47:37	62.29	23.74	8.10	4.78	0.37	0.11	n.d.	0.05	n.d.	99.42	8	2.77	1.25	0.70	0.23	0.02	<0.01	n.d.	<0.01	n.d.	24.57	-	4.97
Bi	cj31:23	34.94	15.64	0.22	0.02	9.81	26.17	6.33	2.39	0.73	96.25	11	2.76	1.46	0.03	<0.01	0.99	1.73	0.74	0.14	0.05	-	0.30	7.90
	cj31:29	35.28	15.38	0.23	0.01	10.01	27.15	5.83	2.49	0.80	97.19	11	2.77	1.42	0.04	<0.01	1.00	1.78	0.68	0.15	0.05	-	0.28	7.90
	cj31:31	34.20	16.30	0.12	n.d.	9.06	26.91	5.97	2.32	0.96	95.84	11	2.71	1.52	0.02	n.d.	0.92	1.78	0.71	0.14	0.06	-	0.28	7.86
	cj31:32	34.27	16.03	0.12	n.d.	9.03	27.12	5.95	2.18	0.93	95.64	11	2.73	1.50	0.02	n.d.	0.92	1.80	0.71	0.13	0.06	-	0.28	7.87
	cj31:33	35.28	15.49	0.18	0.01	10.03	26.43	6.00	2.60	0.85	96.88	11	2.77	1.43	0.03	<0.01	1.01	1.74	0.70	0.15	0.06	-	0.29	7.89
	cj31:34	35.16	15.99	0.09	0.01	9.40	26.72	6.34	2.19	0.98	96.89	11	2.75	1.48	0.01	<0.01	0.94	1.75	0.74	0.13	0.07	-	0.30	7.87
	cj31:35	34.28	15.81	0.11	n.d.	9.70	25.59	5.93	2.22	0.74	94.37	11	2.76	1.50	0.02	n.d.	1.00	1.72	0.71	0.13	0.05	-	0.29	7.88
	cj31:37	34.50	15.81	0.15	n.d.	9.56	25.97	5.97	2.19	0.77	94.91	11	2.76	1.49	0.02	n.d.	0.98	1.74	0.71	0.13	0.05	-	0.29	7.88
	cj47:1	34.59	16.22	0.10	n.d.	9.85	27.02	5.60	2.54	0.35	96.26	11	2.73	1.51	0.02	n.d.	0.99	1.79	0.66	0.15	0.02	-	0.27	7.87
	cj47:3	35.06	16.39	0.18	n.d.	10.11	27.32	5.92	2.45	0.40	97.82	11	2.73	1.50	0.03	n.d.	1.00	1.78	0.69	0.14	0.03	-	0.28	7.90
	cj47:4	34.45	16.17	0.08	0.06	9.80	26.92	5.55	2.58	0.42	96.03	11	2.73	1.51	0.01	0.01	0.99	1.78	0.66	0.15	0.03	-	0.27	7.86
	cj47:6	34.61	16.09	0.22	n.d.	9.83	26.99	5.84	2.56	0.47	96.61	11	2.73	1.50	0.03	n.d.	0.99	1.78	0.69	0.15	0.03	-	0.28	7.90
	cj47:8	33.76	16.14	0.20	0.04	8.74	27.40	5.83	2.35	0.46	94.91	11	2.71	1.52	0.03	<0.01	0.89	1.84	0.70	0.14	0.03	-	0.27	7.86
	cj47:13	33.66	16.07	n.d.	0.01	9.34	27.89	5.53	2.58	0.43	95.51	11	2.70	1.52	n.d.	<0.01	0.96	1.87	0.66	0.16	0.03	-	0.26	7.89
	cj47:16	34.58	16.52	0.22	n.d.	10.05	27.42	5.40	2.61	0.49	97.29	11	2.71	1.53	0.03	n.d.	1.01	1.80	0.63	0.15	0.03	-	0.26	7.90
	cj47:17	34.10	16.37	0.20	n.d.	10.06	27.45	5.32	2.92	0.49	96.89	11	2.69	1.52	0.03	n.d.	1.01	1.81	0.63	0.17	0.03	-	0.26	7.91
	cj47:18	34.18	16.22	0.14	n.d.	10.00	27.46	5.31	2.81	0.48	96.60	11	2.71	1.52	0.02	n.d.	1.01	1.82	0.63	0.17	0.03	-	0.26	7.91
	cj47:19	34.42	16.55	0.09	n.d.	10.12	27.52	5.67	2.79	0.39	97.55	11	2.70	1.53	0.01	n.d.	1.01	1.80	0.66	0.16	0.03	-	0.27	7.91
	cj47:20	34.30	16.41	0.16	0.01	9.89	27.42	5.57	2.93	0.48	97.18	11	2.70	1.52	0.03	<0.01	0.99	1.80	0.65	0.17	0.03	-	0.27	7.89
	cj47:21	34.27	16.75	0.20	n.d.	9.77	27.33	5.92	2.41	0.36	96.99	11	2.69	1.55	0.03	n.d.	0.98	1.80	0.69	0.14	0.02	-	0.28	7.91
	cj47:23	34.38	16.56	0.18	n.d.	9.96	27.27	5.85	2.37	0.42	96.96	11	2.71	1.54	0.03	n.d.	1.00	1.80	0.69	0.14	0.03	-	0.28	7.92
	cj47:24	33.75	16.46	0.08	0.04	9.43	27.76	5.80	2.52	0.42	96.26	11	2.68	1.54	0.01	<0.01	0.96	1.84	0.69	0.15	0.03	-	0.27	7.90

App. I cont.

Min.	oxide/element	SiO_2	Al_2O_3	CaO	FeO	MgO	TiO_2	MnO	Tot.	O	Si	Al	Na	Ca	Fe	Mg	Ti	Mn	Tot.
	Analyse nb.	Country gneisses cont.																	
Grt	cj31:1	35.73	20.48	2.02	21.09	0.45	n.d.	21.83	101.60	12	2.92	1.97	0.02	0.18	1.44	0.05	n.d.	1.51	8.10
	cj31:2	35.28	20.33	2.14	21.30	0.55	n.d.	21.38	100.98	12	2.91	1.98	0.02	0.19	1.47	0.07	n.d.	1.49	8.13
	cj31:3	35.42	20.55	2.17	21.04	0.47	n.d.	21.18	100.81	12	2.91	1.99	0.01	0.19	1.45	0.06	n.d.	1.48	8.09
	cj31:4	35.29	20.34	2.36	21.46	0.53	n.d.	21.17	101.15	12	2.90	1.97	n.d.	0.21	1.48	0.07	n.d.	1.48	8.10
	cj31:6	35.84	20.31	2.32	21.33	0.55	0.01	21.45	101.81	12	2.92	1.95	n.d.	0.20	1.46	0.07	<0.01	1.48	8.08
	cj31:7	35.79	20.83	2.03	20.94	0.49	0.09	22.09	102.26	12	2.91	2.00	0.02	0.18	1.42	0.06	0.01	1.52	8.10
	cj31:8	35.68	20.22	2.37	20.95	0.47	0.03	22.19	101.92	12	2.91	1.95	0.01	0.21	1.43	0.06	<0.01	1.54	8.10
	cj31:10	35.98	20.89	2.25	20.63	0.53	n.d.	22.43	102.72	12	2.90	1.99	0.02	0.20	1.39	0.06	n.d.	1.53	8.09
	cj31:11	35.79	20.24	2.43	21.55	0.48	n.d.	21.28	101.77	12	2.92	1.95	0.02	0.21	1.47	0.06	n.d.	1.47	8.10
	cj31:14	34.99	19.76	2.21	21.44	0.50	n.d.	21.32	100.22	12	2.90	1.93	0.02	0.20	1.49	0.06	n.d.	1.50	8.10
	cj47:1	35.82	20.69	1.89	27.65	1.12	n.d.	14.60	101.77	12	2.91	1.98	0.01	0.17	1.88	0.14	n.d.	1.01	8.09
	cj47:2	36.00	20.92	1.64	27.76	1.02	n.d.	14.88	102.22	12	2.92	2.00	0.01	0.14	1.88	0.12	n.d.	1.02	8.09
	cj47:3	36.05	21.19	2.03	27.50	1.07	n.d.	14.59	102.43	12	2.91	2.02	0.01	0.18	1.86	0.13	n.d.	1.00	8.09
	cj47:4	36.07	21.09	2.19	27.75	1.02	n.d.	14.23	102.34	12	2.91	2.01	0.01	0.19	1.87	0.12	n.d.	0.97	8.08
	cj47:6	36.18	21.09	2.06	28.52	1.17	0.09	13.72	102.82	12	2.91	2.00	0.01	0.18	1.92	0.14	0.01	0.93	8.08
	cj47:7	35.73	21.08	2.15	28.68	1.26	n.d.	12.98	101.88	12	2.90	2.02	0.02	0.19	1.95	0.15	n.d.	0.89	8.11

Appendix II. Modal compositions of the studied granitoids

The amount of each mineral is presented in vol. %.
TGG- Tåghusa gneissic granitoids; LG- Leucogranite; PG- Porphyritic granites; CR- Country rocks; Qz-quartz; Mi- microcline; Pl- plagioclase; Op- opaques; Ti- titanite; Ap-apatite; Ep- epidote; Amph- amphibole; Zr-zircon; Grt- garnet; + -less than 0.5 %; - - 0 %.

	Mineral	Qz	Mi	Pl	Op	Ti	Bi	Ap	Ep	Amph	Zr	Grt	Others	Counts
	Sample													
TGG	cj04	29	23.5	39.7	3	-	3.5	+	0.6	-	-	-	-	> 750
	cj26	27.1	29.4	35	2.7	+	3.4	-	1.7	-	-	-	-	1500
	cj39	32.0	30.9	24.3	3.9	0.7	7.5	-	-	-	-	-	-	800
	cj46	27.2	28.5	25.7	1.6	+	4.6	-	1.2	10.3	-	-	-	1500
LG	cj14	38	37.1	21.6	1.4	-	0.8	-	0.8	-	-	-	-	1500
PG	cj02a	28.2	40	23.1	2.9	+	2.3	0.6	2.3	-	+	-	-	1500
	cj13	23.9	18.7	50.8	3.2	-	2.7	-	-	+	-	-	-	1033
	cj16	20.9	34.7	34.4	1.4	-	8.4	-	-	-	-	-	-	1296
	cj17	29.3	38.7	22.8	2.7	0.5	1.9	+	3.3	-	-	-	-	> 750
	cj20	25.4	30	32.6	5.2	-	4.6	+	1.8	-	-	-	-	1500
	ac29-b	23.9	31.8	33.6	4	0.3	4.2	+	1.2	-	-	-	-	> 750
	cj43	28.5	22.1	42.3	2	-	3.9	-	-	0.7	-	-	-	1113
	cj44	26.3	26.8	39.1	1.9	0.7	3.5	+	1.1	-	-	-	-	> 750
	cj58a	24.7	44	25.8	3.5	-	1.7	-	-	-	-	-	-	1397
CR	cj29	48.9	20.1	25	+	-	5.2	-	0.3	-	-	-	+	1750
	cj30	38.1	33.9	19.6	0.6	-	7.4	-	-	+	-	-	-	1049
	cj31	36.4	33.7	26.1	+	-	3.1	+	+	-	-	-	+	1700
	cj41	29.3	44.3	21.8	0.8	-	3.3	-	+	-	-	-	-	1600
	cj42	31.7	39.2	24.2	0.6	-	1.7	-	+	-	-	-	-	> 750
	cj47	6.95	37.5	44.6	1.95	-	8	0.15	+	-	-	5	+	1025

Appendix III. Chemical analyses of the studied rocks

TGG- Tåghusa gneissic granitoids; LG- Leucogranite; PG- Porphyritic granites; CR- Country rocks

	TGG			LG	PG				CR		
Sample	cj26	cj39	cj46	cj14	cj02	Cj20	cj43	cj58a	cj29	cj41	cj47
Oxide (wt. %)											
SiO_2	70.77	71.80	66.96	76.69	71.77	69.46	71.61	70.26	76.85	75.27	66.10
Al_2O_3	13.67	13.91	13.88	12.20	13.21	14.07	13.52	13.96	12.18	12.90	17.49
Fe_2O_3	3.72	2.75	5.78	1.22	2.84	3.66	2.86	3.53	1.28	1.56	2.72
MgO	0.61	0.46	0.98	0.16	0.42	0.78	0.70	0.56	0.34	0.19	0.42
CaO	1.62	1.31	2.73	0.36	1.27	1.65	1.23	1.71	0.82	0.57	1.52
Na_2O	3.10	3.18	3.34	2.59	2.71	3.16	2.79	2.79	2.98	3.12	4.07
K_2O	4.79	4.71	4.85	5.98	6.31	4.36	5.15	4.87	4.11	5.46	6.21
TiO_2	0.65	0.54	1.02	0.30	0.58	0.73	0.57	0.68	0.21	0.24	0.37
P_2O_5	0.17	0.11	0.28	0.01	0.15	0.18	0.11	0.16	0.05	0.06	0.04
MnO	0.07	0.05	0.11	0.03	0.07	0.08	0.06	0.07	0.03	0.04	0.11
Cr_2O_3	<0.001	<0.001	0.006	<0.001	<0.001	0.007	0.008	0.008	<0.001	<0.001	0.001
LOI	0.40	0.60	0.40	0.60	0.90	0.90	0.60	0.30	0.80	0.40	0.80
Total	99.69	99.54	100.45	100.19	100.36	99.17	99.31	99.01	99.69	99.86	99.93
Element (ppm)											
Ba	1081	1060	1010	497	1140	1169	967	1078	341	433	711
Co	50.8	57.9	54.8	67.8	54.3	43.4	41.8	46.5	75.5	52.9	43.2
Cs	2	1.1	1.5	1.2	1.6	1.6	2.2	0.9	3.1	1.3	1.3
F	1000	420	1200	270	700	1000	930	900	250	400	600
Ga	17.5	17.6	21.5	15.3	17.9	17.2	19.3	19.3	13.8	14.6	29.2
Hf	9	8.6	11.2	6.2	10.8	10.4	10.1	11.6	7.1	7.1	9.1
Nb	18.58	16.19	21.34	21.07	18.52	17.22	18.4	18.6	13.17	13.26	43.89
Rb	205.64	188.42	187.83	312.69	246.18	193.08	241.4	191.6	125.69	189.7	224.9
Sc	6	6	9	3	5	6	6	9	4	2	9
Sn	5.5	4.9	7.3	7.5	6.3	5.1	14	5	4.4	4.1	4.1
Sr	163.9	145.7	187.7	41.8	145.9	161.3	136.1	163.5	71.8	72.6	131
Ta	1.5	1.6	1.5	2	1.7	1.3	1.3	1.2	0.5	0.9	1.5
Th	19.1	17.5	14.7	30	17.3	13.2	19.4	17.2	23.4	12.2	75.8
Tl	0.7	0.6	0.4	1.1	1	0.9	1.7	1.4	0.6	0.8	0.5
U	5	3.8	3.1	8.5	2.9	3.8	4.4	3.5	4.5	1.4	30.1
V	45	44	37	2.5	13	33	19	21	21	11	15
Y	59.5	31.8	67.6	35.6	48.2	41.3	31.7	61.8	64.5	41.5	52.4
Zr	339.5	309.1	448.7	193.9	390.4	416.2	362.5	429.5	247	245.3	281.7
La	88.8	70.9	75.1	56.1	59.6	75.7	59.2	75.4	60.2	53.2	83.9
Ce	166.9	120.7	145.9	107.8	118.3	131.7	117.1	158.1	112.1	107.3	155.3
Pr	21.55	15.07	18.63	12.88	14.23	16.7	11.62	18.53	13.37	11.7	20.52
Nd	81.5	52.9	71.1	43.1	51.5	61.9	40	68.8	48	42.9	74.5
Sm	14.4	8.8	13.4	6.7	9.2	10.3	7.3	13.5	7.7	7.3	13.3
Eu	2.24	1.66	2.45	0.7	1.69	1.82	1.13	2.31	0.51	0.42	1.53
Gd	12.18	6.54	12.08	5.29	8.09	7.9	5.27	11.62	7.28	5.65	10.6
Tb	1.93	1.08	2.01	0.94	1.38	1.21	0.9	1.71	1.26	1.03	1.65
Dy	10.93	6.25	11.71	6.04	8.45	7.26	6.45	12	7.78	6.85	9.36
Ho	2.21	1.22	2.42	1.32	1.85	1.41	1.19	2.21	1.98	1.46	1.86
Er	6.52	3.49	7.28	4.44	5.54	4.3	3.57	6.75	6.23	4.64	5.43
Tm	1.12	0.58	1.26	0.77	0.98	0.75	0.63	1.05	1.16	0.79	0.86
Yb	6.93	4.02	7.49	5.01	6.24	4.4	4.05	6.72	6.63	4.65	4.97
Lu	1.01	0.59	1.08	0.76	0.94	0.68	0.68	1.05	1.11	0.6	0.77
Mo	<1	<1	<1	<1	<1	<1	<1	<1	<1	<1	2
Cu	<1	<1	<1	1	<1	<1	<1	<1	54	3	<1
Pb	10	9	13	63	5	123	3	4	53	9	18
Zn	68	48	66	36	50	75	52	62	32	37	51
Ni	1	1	2	<1	1	1	<1	1	<1	<1	<1
As	<2	<2	<2	<2	<2	<2	<2	<2	<2	<2	<2
Cd	<0.2	<0.2	<0.2	<0.2	<0.2	<0.2	<0.2	<0.2	<0.2	<0.2	<0.2
Sb	<0.5	<0.5	<0.5	<0.5	<0.5	<0.5	<0.5	<0.5	<0.5	<0.5	<0.5
Bi	0.9	<0.5	0.8	<0.5	0.7	0.9	<0.5	0.8	<0.5	<0.5	<0.5

Appendix IV. CIPW norms of the analysed rocks

TGG- Tåghusa gneissic granitoids; LG- Leucogranite; PG- Porphyritic granites; CR- Country rocks

	TGG			LG	PG				CR		
Sample	cj26	cj39	cj46	cj14	cj02	cj20	cj43	cj58a	cj29	cj41	cj47
Oxides- wt. %											
SiO2	70.77	71.8	66.96	76.69	71.77	71.63	71.61	69.46	76.85	75.27	66.1
TiO2	0.65	0.54	1.02	0.3	0.58	0.71	0.57	0.73	0.21	0.24	0.37
Al2O3	13.67	13.91	13.88	12.2	13.21	13.96	13.52	14.07	12.18	12.9	17.49
Fe2O3	0.51	0.38	0.79	0.17	0.39	0.49	0.39	0.5	0.18	0.21	0.37
FeO	2.89	2.14	4.49	0.95	2.21	2.76	2.22	2.84	0.99	1.21	2.11
MnO	0.07	0.05	0.11	0.03	0.07	0.07	0.06	0.08	0.03	0.04	0.11
MgO	0.61	0.46	0.98	0.16	0.42	0.6	0.7	0.78	0.34	0.19	0.42
CaO	1.62	1.31	2.73	0.36	1.27	2.41	1.23	1.65	0.82	0.57	1.52
Na2O	3.1	3.18	3.34	2.59	2.71	4.2	2.79	3.16	2.98	3.12	4.07
K2O	4.79	4.71	4.85	5.98	6.31	1.78	5.15	4.36	4.11	5.46	6.21
P2O5	0.17	0.11	0.28	0.01	0.15	0.15	0.11	0.18	0.05	0.06	0.04
CIPW norm-wt. %											
Qz	29.05	31.26	20.47	37.43	27.88	29.13	31.49	30.21	41.56	34.35	13.61
Ocl	28.64	28.23	28.83	35.54	37.63	26.34	30.94	29.28	24.6	32.5	37.14
Alb	26.54	27.29	28.42	22.04	23.14	27.34	24	24.02	25.54	26.59	34.85
An	7.01	5.86	8.6	1.76	5.29	7.17	5.47	7.57	3.79	2.45	7.37
Cor	0.86	1.48	0	0.83	0	1.62	1.41	1.4	1.48	0.97	1.42
Di	0	0	2.71	0	0.07	0	0	0	0	0	0
Hyp	5.52	4.01	7.22	1.57	3.95	5.82	4.75	5.12	2.26	2.22	4.26
Mt	0.75	0.55	1.15	0.24	0.57	0.74	0.58	0.71	0.26	0.31	0.55
Ilm	1.25	1.04	1.95	0.57	1.11	1.42	1.1	1.31	0.4	0.46	0.71
Ap	0.4	0.26	0.65	0.01	0.35	0.43	0.26	0.38	0.12	0.14	0.09
XMg	0.34	0.35	0.344	0.31	0.32	0.41	0.44	0.34	0.45	0.27	0.30

Tidigare skrifter i serien "Examensarbeten i Geologi vid Lunds Universitet":

118. Romberg, Ewa, 2000: En sediment och biostratigrafisk undersökning av den tidigare Littorina lagunen vid Barsebäck, SV Skåne, med beskrivning av en Preboreal klimatoscillation.
119. Bergman, Jonas, 2000: Skogshistoria i Söderåsens nationalpark. En pollenanalytisk studie i Söderåsens nationalpark, Skåne.
120. Lindahl, Anna, 2000: En paleoekologisk och paleohydrologisk studie av fuktängar i Bräkneåns dalgång, Bräkne Hoby, Blekinge.
121. Eneroth, Erik, 2000: En paleomagnetisk detaljstudie av Sarekgångsvärmen.
122. Terfelt, Fredrik, 2000: Upper Cambrian trilobite faunas and biostratigraphy at Kakeled on Kinnekulle, Västergötland, Sweden.
123. Sundberg, Sven Birger, 2000: Vattenrening genom komplexbildning mellan järn och humusämnen en litteraturstudie med försök.
124. Sundberg, Sven Birger, 2000: Sedimentationsprocesser och avlagringsmiljö för en kantrygg kring platåleran vid Rydsgårds gods i backlandskapet söder om Romeleåsen, Skåne.
125. Kjöllerström, Anders, 2000: En geokemisk studie av bergartsvariationen på Bullberget i västra Dalarna.
126. Cinthio, Kajsa, 2000: Senglacial och tidigholocen etablering och expansion av lövträd på en lokal i nordvästra Rumänien.
127. Lamme, Sara, 2000: Klimat och miljöförändringar under holocen i Sylarnaområdet, södra svenska Skanderna, baserat på analys av makrofossil och klyvöppningar.
128. Jönsson, Charlotte, 2000: Geologisk och hydro-geologisk modellering av området mellan Bjuv och Söderåsen, nordvästra Skåne.
129. Kleman, Johan, 2001: Utvärdering av den underkambriska litostratigrafin på Österlen, södra Sverige.
130. Sundler, Malin, 2001: En jämförande studie mellan uppmätt och MACRO simulerad pesticidutlakning på ett odlingsfält i Skåne.
131. Grönholm, Anna, 2001: Högtrycksmetabasiter i den södra delen av Mylonitzonen: fältgeologi, petrografi och metamorf utveckling.
132. Ekdahl, Magnus, 2001: En studie av Källsjögranitens deformationsmönster och kinematiska indikatorer inom Ullaredszonen.
133. Axheimer, Niklas, 2001: Middle Cambrian trilobites and biostratigraphy of the Almbacken drill core, Scania, Sweden.
134. Lindén, Mattias, 2001: Proglacial deformation of glaciofluvial sediments during the Pomeranian deglaciation in the Neubrandenburg area, NE Germany.
135. Warnhag, Jon, 2001: A geochemical study of the zoned Pan African Mon Repos intrusion, Central Namibia.
136. Lundmark, Mattias, 2001: Zirkonstudie av Norra Hortens bergarter, SV Sverige.
137. Gunnarson, Rebecka, 2001: Sedimentologisk undersökning av en moränskärning i en djup-vittrad sprickdal på Romeleåsen, Skåne.
138. Karlsson, Christine, 2001: Diagenetic and petro-physical properties of deeply versus moderately buried Cambrian sandstones of the Caledonian foreland, southern Sweden.
139. Eriksson, Mårten, 2001: Bedömning av föroreningsspridning kring en nedlagd bensinstation i Karlaby, sydöstra Skåne.
140. Ljung, Karl, 2001: A paleoecological study of the Pleistocene Holocene transition in the Kap Farvel area, South Greenland.
141. Åkesson, Cecilia, 2001: Undersökning av grundvattenförhållanden i området kring Östra Vemmerlöv, Simrishamns kommun, sydöstra Skåne.
142. Bermin, Jonas, 2001: Modelling Mössbauer spectra of biotite.
143. Mansurbeg, Howri, 2001: Modelling of reservoir quality in quartz-rich sandstones of the Lower Cretaceous Bentheim sandstones, Lower Saxony Basin, NW Germany.
144. Hermansson, Tobias, 2001: Sierggavággeskollans strukturgeologiska utveckling; nyckeln till Sareks berggrundsgeologi.
145. Veres, Daniel-Stefan, 2001: A comparative study between loss on ignition and total carbon analysis on Late Glacial sediments from Atteköps mosse, southwestern Sweden, and their tentative correlation with the GRIP event stratigraphy.
146. Ahlberg, Tomas, 2001: Hydrogeologisk undersökning samt sårbarhetskartering av området kring tre bergborrade grundvattenanläggningar i Simrishamns kommun.
147. Boman, Daniel, 2001: Tektonostratigrafi och deformationsrelaterad metamorfos i norra Kebnekaisefjällen, Skandinaviska Kaledo-

niderna.

148. Olsson, Stefan, 2002: The geology of the Portobello Peninsula; proposal of a saturated to oversaturated lineage within the Dunedin Volcano, New Zealand.

149. Molnos, Imre, 2002: Petrografi och diagenes i den underkambriska lagerföljden i Skrylle, Skåne.

150. Malmborg, Pär, 2002: Correlation between diagenesis and sedimentary facies of the Bentheim Sandstone, the Schoonebeek field, The Netherlands.

151. Jonsson, Henrik, 2002: Permeability variation in a tidal Jurassic deposit, Höganäs basin, Fennoscandian Border Zone

152. Lundgren, Anders, 2002: Seveskollorna i nord-östra Kebnekaise, Kaledoniderna: metabasiter, graniter och ögongnejser.

153. Sultan, Lina, 2002: Reconstruction of fan-shaped outwash in front of the Mýrdalsjökull ice cap, Iceland: Architecture and style of sedimentation.

154. Rimša, Andrius, 2002: Petrological study of the metamafic rocks across the Småland-Blekinge Deformation Zone

155. Lund, Magnus, 2002: Anti-slope scarp investigation at Handcar Peak, British Columbia, Canada.

156. Sjöstrand, Lisa: 2003: Early to early Middle Ordovician conodont biostratigraphy of the Tamsalu drill core, central Estonia.

157. Nilsson, Jonas, 2003: Carcharhiniforma hajar från Limhamns kalkbrott.

158. Larsson, Linda M., 2003: Late Triassic and Early Jurassic palynology of the Höganäs Basin and the Ängelholm Trough, NW Scania, Sweden.

159. Sköld, Pia, 2003: Holocen skogshistoria i Stenshuvuds nationalpark, Skånes östra kust, Sverige.

160. Fuchs, M., 2003: Påverkan av sterilisering på gruvsand – en mineralogisk och texturell undersökning.

161. Ljungberg, Julia, 2003. Sierggavágge-skollan i gränslandet mellan Sarek och Padjelanta; miljöindikatorer för fjällkedjeberggrundens bildning.

162. Håkansson, Lena, 2003: An architectural element analysis of a large-scale thrust complex, Kanin Peninsula, NW Russia: interaction between the Barents and Kara Sea ice sheets.

163. Davidson, Anja, 2003: Ignimbritenheterna i Barranco de Tiritaña, övre Mogánformationen, Gran Canaria.

164. Näsström, Helena, 2003: Klotdioriten vid Slättemossa, centrala Småland – mineralkemi och genes.

165. Nilsson, Andreas, 2003: Early Ludlow (Silurian) graptolites from Skåne, southern Sweden.

166. Dou, Marion, 2003: Les ferromagnésiens du granite rapakivique de Nordingrå – centre-est de la Suède – composition chimique et stade final de cristallisation.

167. Jönsson, Emma, 2003: En pollenanalytisk studie av råhumusprofiler från Säröhalvön i norra Halland.

168. Alwmark, Carl, 2003: Magmatisk och metamorf petrologi av en mafisk intrusion i Mylonitzonen.

169. Pettersson, Ann, 2003: Jämförande litologisk och geokemisk studie av Sevens amfibolitkomplex i Sylarna och Kebnekaise.

170. Axelsson, Katarina, 2004: Bedömning av potentiell föroreningsspridning från ett avfallsupplag utanför Löddeköpinge, Skåne.

171. Ekestubbe, Jonas, 2004: $^{40}Ar/^{39}Ar$ geokronologi och implikationer för tolkningen av den Kaledoniska utvecklingen i Kebnekaise.

172. Lindgren, Paula, 2004. Tre sensvekofenniska graniter: kontakt- och åldersrelationer samt förekomst av metasedimentära enklaver.

173. Janson, Charlotta, 2004. A petrographical and geochemical study of granitoids from the south-eastern part of the Linderödsåsen Horst, Skåne.

LUNDS UNIVERSITET

Geologiska institutionen
Gentrum för GeoBiosfärsvetenskap
Sölvegatan 12, 223 62 Lund